PHYSICAL REVIEW D **80,** 094021 (2009)

Two-pseudoscalar-meson decay of χ_{cJ} with twist-3 corrections

Ming-Zhen Zhou[†]

School of Physical Science and Technology, Southwest University, Chongqing 400715, People's Republic of China[*]

Hai-Qing Zhou[‡]

Department of Physics, Southeast University, Nanjing 211189 China

(Received 15 October 2009; published 30 November 2009)

The decays of $\chi_{cJ} \to \pi^+\pi^-$, K^+K^- $(J = 0, 2)$ are discussed within the standard and modified hard-scattering approach when including the contributions from twist-3 distribution amplitudes and wave functions of the light pseudoscalar meson. A model for twist-2 and twist-3 distribution amplitudes and wave functions of the pion and kaon with BHL prescription are proposed as the solution to the end-point singularities. The results show that the contributions from twist-3 parts are actually not power suppressed comparing with the leading-twist contribution. After including the effects from the transverse momentum of light meson valence-quark state and Sudakov factors, the decay widths of the χ_{cJ} into pions or kaons are comparable with the their experimental data.

DOI: 10.1103/PhysRevD.80.094021 PACS numbers: 14.40.Gx, 21.30.Fe, 25.40.Ve, 25.70.Ef

I. INTRODUCTION

The factorization form in the framework of the hard-scattering picture [1] is usually used in hadronic processes with large momentum transfer. In this picture, the full amplitude is factorized as a convolution of process independent distribution amplitudes of hadrons and process-dependent hard-scattering amplitude. However, the applicability of this approach at experimentally accessible momentum transfers, typically a few GeV, is questionable [2]. One of the reasons is the large contributions from the soft end-point regions. A modified perturbative approach, so-call modified hard-scattering approach (mHSA), has been proposed by Li and Sterman [3], where quark transverse momenta and Sudakov suppressions are taken into account. The advantage of this modified perturbative approach is the strong suppression of the soft end-point regions where the pQCD can not be applied.

The exclusive charmonium decays have attracted interest for decades as they are an excellent laboratory for studying quark-gluon dynamics at relatively low energies. In the decay of P-wave charmonium $\chi_{c0,2}$ to a pair of pseudoscalars, one finds that the lowest Fock state, the color-singlet contribution, alone is not sufficient to accommodate the experimental data. This discrepancy provides an important arena in which to test our understanding of the boundary domain between perturbative and nonperturbative QCD. From a naive point of view, QCD radiative correction is suppressed by the factor $\alpha_s(Q^2)$ and the contribution from higher Fock states, higher twist distribution amplitudes are suppressed by the factor $1/Q^2$. But this is not always the real case. In Ref. [4], the author showed that in the decay of $\chi_{c0,2} \to PP$ (where P represents a light pseudoscalar meson.) the color-octet contribution from the higher Fock state contributes the same level as the color-singlet state.

To reveal the decay mechanism more clear, the systemic reanalysis on the contributions from higher twist distribution amplitudes will be significative and interested. When the amplitude of a physical process with large momentum transfer Q^2 is only related to one hadron wave function, there is a suppression for the contribution from higher Fock states and higher twist distribution amplitudes. For example, the dominating contribution of $\pi - \gamma$ transition form factor [5] comes from the leading-twist distribution amplitude of valence-quark state. The QCD correction is only about 10%–20% [6] and corrections from higher Fock state and higher twist distribution amplitudes [7] are suppressed by additional powers of $1/Q^2$. However, for the exclusive processes with the overlap of the wave functions of the initial hadron and final hadrons there are a lot of space to discuss the contributions from higher twist terms. For instance, the contribution of twist-3 distribution amplitudes to the pion electromagnetic form factor is comparable and even larger than the contribution from the leading-twist distribution amplitude of the pion at intermediate energy region of Q^2, being 2–40 GeV^2 in Ref. [8]. The similar result has also been obtained for the kaon electromagnetic form factor in Ref. [9]. More discussion about the contributions from the higher twist distribution amplitudes can be found in the Heavy-to-light transition form factors [10], the nonleptonic two-body decays of the B meson [11], and so on.

In this paper, we apply both the mHSA and the sHSA to reexamine the decay of $\chi_{cJ} \to \pi^+\pi^-$, K^+K^- $(J = 0, 2)$ including the contribution from the two-particle twist-3 wave functions and distribution amplitudes of the light pseudoscalar meson. In the sHSA case, the end-point

[*]Mailing address.
[†]zhoumz@mail.ihep.ac.cn
[‡]zhouhq@mail.ihep.ac.cn

singularity can be avoided by using the BHL prescription [12] in which the light meson distribution amplitudes are rewritten with exponential suppression factors. Our results show that the contributions from twist-3 wave function are comparable with or even larger than the leading-twist contribution. Comparing with [4], the present analysis has an advantage that the theoretical uncertainty from light meson higher twist wave functions is less than that from the color-octet wave function and the constituent gluon from the octet state of the charmonium. One can find the discussion on light meson twist-3 wave functions in many literatures [13–15].

The paper is organized as following. In Sec. II the main calculation of the hard-scattering amplitude in the modified perturbative QCD approach is presented. In Sec. III, we present our model for the light meson two-particle twist-2 and twist-3 wave functions and the distribution amplitude within the BHL scheme. The Sec. IV is the numerical analysis and Sec. V is our conclusion. The coefficients of hard-scattering amplitudes in the momentum space and in the b space are given in Appendix A and B. The Sudakov factor is presented in Appendix C.

II. CALCULATION OF HARD-SCATTERING AMPLITUDES

The two-meson decays of χ_{cJ} can be described as $c\bar{c}$ quarks annihilate into two gluons and then materializing into two final-state mesons as illustrated in Fig. 1. We work in the rest frame of χ_{cJ} meson and take approximation $M = 2m_c$ where M is the mass of the charmonium meson and m_c is the mass of c-quark. The masses of pion and kaon are canceled in the Chiral limit. Under these conventions, the momentums of the initial- and final-state mesons are described in terms of light-cone variables as

$$P=\left(\frac{M}{\sqrt{2}},\frac{M}{\sqrt{2}},0_T\right),\quad p_1=\left(\frac{M}{\sqrt{2}},0,0_T\right),\quad p_2=\left(0,\frac{M}{\sqrt{2}},0_T\right), \tag{1}$$

where P is the momentum of the charmonium and p_1 and p_2 are the momentums of $\pi^+(K^+)$ and $\pi^-(K^-)$, respectively. In the following, we only present the two-pion decay of χ_{cJ} for the two-kaon decay is similar.

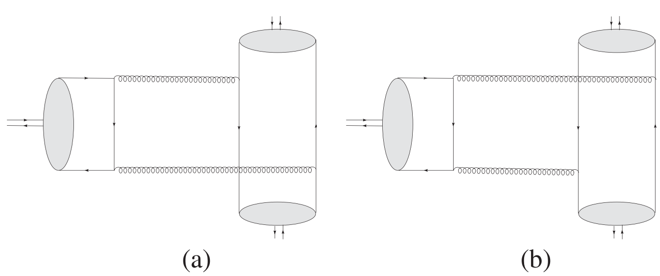

FIG. 1. The hard-scattering diagrams for the decay $\chi_{cJ} \to \pi^+\pi^-$, K^+K^- $(J = 0, 2)$.

For the two-pion decay of χ_{cJ}, its decay width can be written as:

$$\Gamma[\chi_{cJ} \to \pi^+\pi^-] = \frac{1}{16\pi M}\frac{1}{2J+1}\sum_{J_z}|\mathcal{M}(\chi_{cJ} \to \pi^+\pi^-)|^2, \tag{2}$$

where $\mathcal{M}$ is the transitional matrix element. As usual, this matrix element within the mHSA can be factorized as the convolution with respect to the momentum fractions x, y and transverse separation scales $\mathbf{b}_1$, $\mathbf{b}_2$ of the two pions,

$$\mathcal{M}(\chi_{cJ} \to \pi^+\pi^-) = \int_0^1 dxdy \int \frac{d^2\mathbf{b}_1}{4\pi}\frac{d^2\mathbf{b}_2}{4\pi}\sum_{i,j}\Psi_i(y,\mathbf{b}_2) \times \mathcal{T}^{ij}_{HJ}(x,y,\mathbf{b}_1,\mathbf{b}_2)\Psi_j(x,\mathbf{b}_1) \times e^{-S(x,y,\mathbf{b}_1,\mathbf{b}_2,t_1,t_2)}, \tag{3}$$

here the scripts $(i, j = \pi, p, \sigma)$ mean the twist-2 and twist-3 wave functions for the pion meson and S is the Sudakov factor. $\mathcal{T}^{ij}_{HJ}(x,y,\mathbf{b}_1,\mathbf{b}_2)$ is the Fourier transform of the hard-scattering amplitudes $T^{ij}_{HJ}(x,y,\mathbf{k}_1,\mathbf{k}_2)$

$$\mathcal{T}^{ij}_{HJ}(x,y,\mathbf{b}_1,\mathbf{b}_2) = \int \frac{d^2\mathbf{k}_1}{(2\pi)^2}\frac{d^2\mathbf{k}_2}{(2\pi)^2}T^{ij}_{HJ}(x,y,\mathbf{k}_1,\mathbf{k}_2) \times e^{-i\mathbf{k}_1\cdot\mathbf{b}_1-i\mathbf{k}_2\cdot\mathbf{b}_2}. \tag{4}$$

$T^{ij}_{HJ}(x,y,\mathbf{k}_1,\mathbf{k}_2)$ can be calculated from the graphs shown in Fig. 1 and the scripts of nonzero terms are $ij = \pi\pi$, pp, $p\sigma$, σp, $\sigma\sigma$, $\mathbf{k}_1$ and $\mathbf{k}_2$ are the intrinsic transverse momentum of two final-state pion mesons, respectively.

To calculate the transitional matrix element, the wave functions of the pion meson and the charmonium should be introduced. Similar to the definition of distribution amplitudes with leading and next-to-leading-twist [13], the light-cone wave functions of pion are defined in terms of bilocal operator matrix element

$$\langle\pi(p_\pi)|\bar{q}_\beta(z_1)q_\alpha(z_2)|0\rangle=\frac{if_\pi}{4}\int_0^1 dx\int\frac{d^2\mathbf{k}_\perp}{16\pi^3} \times e^{i(xp_\pi\cdot z_1+(1-x)p_\pi\cdot z_2-\mathbf{k}_\perp\cdot(\mathbf{z}_1-\mathbf{z}_2)_\perp)} \times\Big\{\not{p}_\pi\gamma_5\Psi_\pi(x,\mathbf{k}_\perp)-\mu_\pi\gamma_5 \times\Big(\Psi_p(x,\mathbf{k}_\perp)-\sigma_{\mu\nu}p^\mu_\pi(z_1-z_2)^\nu \times\frac{\Psi_\sigma(x,\mathbf{k}_\perp)}{6}\Big)\Big\}_{\alpha\beta}, \tag{5}$$

where f_π is the decay constant of pion and the parameter $\mu_\pi = m^2_\pi/(m_u + m_d)$ for charged pion. Ψ_π, Ψ_p and Ψ_σ are the twist-2 and twist-3 wave functions, respectively. The twist-3 wave functions contributes power corrections. But at m_c energy scale, the Chirally enhanced parameter $r_\pi = \mu_\pi/m_c \sim 1$ is large enough to consider the twist-3 contributions in charmonium decays.

For simplification, the wave function of the charmonium is taken as [16],

$$\chi(P, q; J, J_z) = \sum_{M,S_z} 2\pi\delta\left(q^0 - \frac{\vec{q}^2}{2m_c}\right) \times \langle LM; SS_z|JJ_z\rangle \psi_{LM}(\vec{q})\mathcal{P}_{SS_z}(P, q), \quad (6)$$

where q is the relative momentum between the quark and antiquark, $\psi_{LM}(\vec{q})$ and $\mathcal{P}_{SS_z}(P, q)$ are the spatial wave function and spin projection operators, respectively. The spin projection operators $\mathcal{P}_{SS_z}(P, q)$ are

$$\mathcal{P}_{SS_z}(P, q) = \sqrt{\frac{3}{8m_c^3}}\left[m_c + \left(\frac{\not{P}}{2} + \not{q}\right)\right] \times \left(1 + \frac{\not{P}}{M}\right)\Pi_{SS_z}\left[m_c - \left(\frac{\not{P}}{2} - \not{q}\right)\right] \quad (7)$$

with $\Pi_{SS_z} = -\gamma_5$ for $S = 0$ and $\Pi_{SS_z} = -\not{\varepsilon}(S_z)$ for $S = 1$. Here $\varepsilon(S_z)$ refers to the spin part of the wave function, $\varepsilon(S_z) = (0, 0, 0, 1)$ for $S_z = 0$ and $\varepsilon(S_z) = (0, \mp 1, -i, 0)/\sqrt{2}$ for $S_z = \pm 1$.

With the definition of the wave functions for the initial- and final-state hadrons, the transition matrix element of the two-pion decay for χ_{cJ} can be calculated in the coordinate space by standard method and then hard-scattering amplitudes $T_{HJ}^{ij}(x, y, \mathbf{k}_1, \mathbf{k}_2)$ can be extracted as

$$T_{HJ}^{ij}(x, y, \mathbf{k}_1, \mathbf{k}_2) = -\frac{32\pi^2}{27}\alpha_s(t_1^2)\alpha_s(t_2^2)\hat{T}_{\mu\nu}^{ij}\int\frac{d^4q}{(2\pi)^4} \times \frac{\mathrm{Tr}[\chi(P, q; J, J_z)\hat{\mathcal{O}}^{\mu\nu}(q)]}{(l_1^2 + i\epsilon)(l_2^2 + i\epsilon)} + (l_1 \leftrightarrow l_2), \quad (8)$$

where $l_1 = xp_1 + yp_2 + \mathbf{k}_1 - \mathbf{k}_2$ and $l_2 = (1 - x)p_1 + (1 - y)p_2 - \mathbf{k}_1 + \mathbf{k}_2$ are the momentum of two intermediate gluons, respectively. The operator $\hat{\mathcal{O}}^{\mu\nu}(q)$, which is related to the two-gluon annihilation of charmonium, reads

$$\hat{\mathcal{O}}^{\mu\nu}(q) = \frac{\gamma^\mu(\not{k}_c + m_c)\gamma^\nu}{k_c^2 - m_c^2 + i\epsilon}, \quad (9)$$

where $k_c = (l_1 - l_2)/2 + q$ is the corresponding momentum of the c-quark propagator. The operators $\hat{T}_{\mu\nu}^{ij}$ are related to the two-meson materialization of two gluons with different twist wave functions and are expressed as

$$\hat{T}_{\mu\nu}^{\pi\pi} = \frac{f_\pi^2}{16}\mathrm{Tr}[\gamma_\mu\not{p}_2\gamma_5\gamma_\nu\not{p}_2\gamma_5],$$
$$\hat{T}_{\mu\nu}^{pp} = \frac{f_\pi^2\mu_\pi^2}{16}\mathrm{Tr}[\gamma_\mu\gamma_5\gamma_\nu\gamma_5],$$
$$\hat{T}_{\mu\nu}^{p\sigma} = -i\frac{f_\pi^2\mu_\pi^2}{4\times 24}\mathrm{Tr}[\gamma_\mu\gamma_5\gamma_\nu\sigma_{\alpha\beta}\gamma_5]p_1^\alpha\left(\frac{\partial}{\partial l_{1\beta}} - \frac{\partial}{\partial l_{2\beta}}\right),$$
$$\hat{T}_{\mu\nu}^{\sigma p} = i\frac{f_\pi^2\mu_\pi^2}{4\times 24}\mathrm{Tr}[\gamma_\mu\sigma_{\alpha\beta}\gamma_5\gamma_\nu\gamma_5]p_2^\alpha\left(\frac{\partial}{\partial l_{1\beta}} - \frac{\partial}{\partial l_{2\beta}}\right),$$
$$\hat{T}_{\mu\nu}^{\sigma\sigma} = -\frac{f_\pi^2\mu_\pi^2}{16\times 36}\mathrm{Tr}[\gamma_\mu\sigma_{\tau\alpha}p_2^\tau\gamma_5\gamma_\nu\sigma_{\delta\beta}p_1^\delta\gamma_5] \times \left(\frac{\partial}{\partial l_{1\alpha}} - \frac{\partial}{\partial l_{2\alpha}}\right)\left(\frac{\partial}{\partial l_{1\beta}} - \frac{\partial}{\partial l_{2\beta}}\right), \quad (10)$$

where the partial $(\frac{\partial}{\partial l_{1\nu}} - \frac{\partial}{\partial l_{2\nu}})$ comes from the $(z_1 - z_2)^\nu$ term of Eq. (5). Here we do not take the momentum projection of Eq. (5), which can be obtained by transforming the parameters in terms of coordinate variable in Eq. (5) into the momentum space configuration, in Ref. [17] or [18].

For P-wave charmonium decay, the dominant contribution is given by q^λ term of $\mathrm{Tr}[\chi(P, q; J, J_z)\hat{\mathcal{O}}^{\mu\nu}(q)]$ and the result after the integration of momentum q can be rewritten as

$$\sum_{M,S_z}\sqrt{\frac{3}{\pi}}\frac{R_p'(0)}{4}\langle 1M, 1S_z|JJ_z\rangle\varepsilon^\lambda(M) \times \mathrm{Tr}[\hat{\mathcal{O}}_\lambda^{\mu\nu}(0)\mathcal{P}_{1S_z}(P, 0) + \hat{\mathcal{O}}^{\mu\nu}(0)\mathcal{P}_{1S_z,\lambda}(P, 0)], \quad (11)$$

with the definition of the partial of the P-wave function at the origin

$$\int\frac{d^3q}{(2\pi)^3}q^\lambda\psi_{1M}(\vec{q}) = \sqrt{\frac{3}{\pi}}\frac{R_p'(0)}{4}\varepsilon^\lambda(M), \quad (12)$$

where $\varepsilon^\lambda(M)$ refers to the orbital part of the wave function and

$$\hat{\mathcal{O}}^{\mu\nu}(0) = \frac{\gamma^\mu[(\not{l}_1 - \not{l}_2)/2 + m_c]\gamma^\nu}{(l_1 - l_2)^2/4 - m_c^2},$$
$$\hat{\mathcal{O}}_\lambda^{\mu\nu}(0) = \frac{\gamma^\mu\gamma_\lambda\gamma^\nu}{(l_1 - l_2)^2/4 - m_c^2} - \frac{(l_1 - l_2)_\lambda\gamma^\mu[(\not{l}_1 - \not{l}_2)/2 + m_c]\gamma^\nu}{[(l_1 - l_2)^2/4 - m_c^2]^2},$$
$$\mathcal{P}_{1S_z}(P, 0) = \sqrt{\frac{3}{8m_c^3}}\left(m_c + \frac{\not{P}}{2}\right)\left(1 + \frac{\not{P}}{M}\right)\Pi_{1S_z}\left(m_c - \frac{\not{P}}{2}\right),$$
$$\mathcal{P}_{1S_z,\lambda}(P, 0) = \sqrt{\frac{3}{8m_c^3}}\left[\gamma_\lambda\left(1 + \frac{\not{P}}{M}\right)\Pi_{1S_z}\left(m_c - \frac{\not{P}}{2}\right) + \left(m_c + \frac{\not{P}}{2}\right)\left(1 + \frac{\not{P}}{M}\right)\Pi_{1S_z}\gamma_\lambda\right]. \quad (13)$$

The final hard-scattering amplitudes with transverse momentum can be expressed as

$$T^I_{HJ}(x, y, \mathbf{k}_1, \mathbf{k}_2) = \frac{16}{9\sqrt{6}} C^I \left(\frac{\mu_\pi^2}{m_c^2}\right)^{t_I - 2} N_0 \sigma_J \times \frac{\alpha_s(t_1^2)\alpha_s(t_2^2)}{D_1^{d_I} D_2^{d_I} N^{n_I}} \sum_{i=0}^{i_I} C_i^I(J) N^i, \quad (14)$$

where $N_0 = 16\pi^{3/2} f_\pi^2 m_c^{5/2} R_p'(0)$, $\sigma_0 = 1$ for χ_{c0} and $\sigma_2 = 1/\sqrt{2}$ for χ_{c2}. The coefficients C^I, t_I, d_I, n_I, i_I are listed in Table I. The virtualities of the internal c-quark and the two intermediate gluons are

$$\begin{aligned} D_1 &= 4m_c^2 xy - \mathbf{K}^2 + i\epsilon, \\ D_2 &= 4m_c^2(1-x)(1-y) - \mathbf{K}^2 + i\epsilon \\ N &= 2m_c^2(x + y - 2xy) + \mathbf{K}^2 - i\epsilon \end{aligned} \quad (15)$$

with $\mathbf{K} = \mathbf{k}_1 - \mathbf{k}_2$. The coefficients $C_0^{\pi\pi}(J) = 1$ and $C_1^{\pi\pi}(J) = (-2)^{J/2} m_c^2 (x-y)^2$ are in agreement with the results from Ref. [4] and the others coefficients are showed in Appendix A.

Next, the fact that hard-scattering amplitudes T^{ij}_{HJ} depend on $\mathbf{k}_1$ and $\mathbf{k}_2$ only in the combination $\mathbf{K}$ implies the following result for the Fourier transform of them

$$\begin{aligned} \mathcal{T}^I_{HJ}(x, y, \mathbf{b}_1, \mathbf{b}_2) = {}& \frac{2}{9\sqrt{6}} C^I \left(\frac{\mu_\pi^2}{m_c^2}\right)^{t_I - 2} \mathcal{N}_0 \sigma_J \delta(\mathbf{b}_1 - \mathbf{b}_2) \\ & \times \alpha_s(t_1^2)\alpha_s(t_2^2)\Bigg[i\Bigg(\sum_{i=0}^{d_I - 1} A^I_{1i}(J) H_i^{(1)}(r_1) \\ & - \sum_{i=0}^{d_I-1} A^I_{2i}(J) H_i^{(1)}(r_2)\Bigg) \\ & + \sum_{i=0}^{n_I - 1} B_i^I(J) K_i(r_3)\Bigg], \end{aligned} \quad (16)$$

where $\mathcal{N}_0 = 16\pi^{3/2} f_\pi^2 R_p'(0)/m_c^{3/2}$, $r_1 = \sqrt{xy} b$, $r_2 = \sqrt{(1-x)(1-y)} b$ and $r_3 = \sqrt{(x + y - 2xy)/2} b$ with $b = 2m_c b_1$. $H_i^{(1)}$ and K_i denote Hankel and modified Bessel functions, respectively. The δ-function, which simplifies the numerical work enormously, means that the two pions emerge from the decay with identical transverse separations. The coefficients $A^I_{1i}(J)$, $A^I_{2i}(J)$ and $B^I_i(J)$ are listed in Appendix B.

The novel ingredient of the mHSA is the Sudakov factor e^{-S}, which takes into account those gluonic radiative

TABLE I. The values of coefficients C^I, t_I, d_I, n_I, and i_I in the Eq. (14).

I	$\pi\pi$	pp	$p\sigma$	σp	$\sigma\sigma$
C^I	1	$\frac{1}{4}$	$\frac{1}{3}$	$\frac{1}{3}$	$\frac{1}{9}$
t_I	2	3	3	3	3
d_I	1	1	2	2	3
n_I	2	2	3	3	4
i_I	1	1	3	3	6

corrections not accounted for in the QCD evolution of the wave function. In next-to-leading-log approximation, the Sudakov exponent reads

$$\begin{aligned} S(x, y, \mathbf{b}_1, \mathbf{b}_2, t_1, t_2) &= s(x, b_1, 2m_c) + s(1-x, b_1, 2m_c) \\ &\quad + s(y, b_2, 2m_c) + s(1-y, b_2, 2m_c) \\ &\quad - \frac{1}{\beta_1} \ln \frac{\ln(t_1/\Lambda_{\mathrm{QCD}}) \ln(t_2/\Lambda_{\mathrm{QCD}})}{\ln(1/(b_1\Lambda_{\mathrm{QCD}})) \ln(1/(b_2\Lambda_{\mathrm{QCD}}))}, \end{aligned} \quad (17)$$

where the function $s(x, b_i, Q)$ with next-to-leading-log correction is given in Appendix C. The last term in Eq. (17) arises from a renormalization group transformation from the factorization scales μ_{Fi} to the renormalization scales t_j at which the hard-scattering amplitudes $\mathcal{T}^I_{HJ}(x, y, \mathbf{b}_1, \mathbf{b}_2)$ are evaluated.

The renormalization scales appearing in α_s and in the Sudakov exponent are chosen as

$$\begin{aligned} t_1 &= \max\{2m_c\sqrt{xy}, 1/b_1, 1/b_2\}, \\ t_2 &= \max\{2m_c\sqrt{(1-x)(1-y)}, 1/b_1, 1/b_2\} \end{aligned} \quad (18)$$

by the virtualities of the intermediate gluons, which depend nontrivially on the integration variables. This choice of the renormalization scale avoids large logs from higher-order pQCD. The factorization scale is given by the quark-antiquark separation $\mathbf{b}_i$, $\mu_{Fi} = 1/b_i$. The ratio $1/b_i$ marks the interface between nonperturbatively soft momenta, which are implicitly accounted for in the pion wave functions, and the contributions from semihard gluons, incorporated in a perturbative way in the Sudakov factor.

Replacing e^{-S} by 1 and ignoring the transverse momenta in $T^I_{HJ}(x, y, \mathbf{k}_1, \mathbf{k}_2)$, one finds the decay amplitude within the sHSA as derived by Duncan and Mueller [19],

$$\mathcal{M}(\chi_{cJ} \to \pi^+\pi^-) = \sum_{i,j}^{\pi,p,\sigma} \int_0^1 dx \int_0^1 dy \phi_i(x, \mu_F) \times T^{ij}_{HJ}(x, y, m_c^2) \phi_j(y, \mu_F), \quad (19)$$

where the renormalization scale t_j is taken as the charm-quark mass and customarily identified with the factorization scale. The hard-scattering amplitudes $T^{ij}_{HJ}(x, y, m_c^2)$ are expressed as follows

$$
\begin{aligned}
T_{H0}^{\pi\pi}(x,y,m_c^2) &= \frac{\mathcal{N}_0\alpha_s^2(m_c^2)}{36\sqrt{6}m_c^2}\frac{x^2+(2-6y)x+y(y+2)}{x(1-x)y(1-y)(x+y-2xy)^2},\\
T_{H0}^{pp}(x,y,m_c^2) &= \frac{\mathcal{N}_0\alpha_s^2(m_c^2)}{72\sqrt{6}m_c^2}\frac{\mu_\pi^2}{m_c^2}\frac{x^2+(3-8y)x+y(y+3)}{x(1-x)y(1-y)(x+y-2xy)^2},\\
T_{H0}^{p\sigma}(x,y,m_c^2) &= -\frac{\mathcal{N}_0\alpha_s^2(m_c^2)}{432\sqrt{6}m_c^2}\frac{\mu_\pi^2}{m_c^2}\frac{y^3+x(-2y^2-5y+5)y+x^2(8y^2-8y+1)}{x(1-x)y^2(1-y)^2(x+y-2xy)^3},\\
T_{H0}^{\sigma p}(x,y,m_c^2) &= -\frac{\mathcal{N}_0\alpha_s^2(m_c^2)}{432\sqrt{6}m_c^2}\frac{\mu_\pi^2}{m_c^2}\frac{(1-2y)x^3+y(8y-5)x^2+(5-8y)yx+y^2}{x^2(1-x)^2y(1-y)(x+y-2xy)^3},\\
T_{H0}^{\sigma\sigma}(x,y,m_c^2) &= -\frac{\mathcal{N}_0\alpha_s^2(m_c^2)}{2592\sqrt{6}m_c^2}\frac{\mu_\pi^2}{m_c^2}\frac{1}{x^2(1-x)^2y^2(1-y)^2(x+y-2xy)^4}((24y^3-36y^2+14y-1)x^5\\
&\quad+(48y^4-156y^3+145y^2-42y+3)x^4+y(8y^4-116y^3+218y^2-129y+17)x^3\\
&\quad+y(-12y^4+89y^3-97y^2+24y+4)x^2+y^2(6y^3-26y^2+9y+4)x-(y-3)y^4)
\end{aligned}
\tag{20}
$$

for $J=0$ and

$$
\begin{aligned}
T_{H2}^{\pi\pi}(x,y,m_c^2) &= \frac{\mathcal{N}_0\alpha_s^2(m_c^2)}{36\sqrt{3}m_c^2}\frac{x+y-x^2-y^2}{x(1-x)y(1-y)(x+y-2xy)^2},\\
T_{H2}^{pp}(x,y,m_c^2) &= -\frac{\mathcal{N}_0\alpha_s^2(m_c^2)}{72\sqrt{3}m_c^2}\frac{\mu_\pi^2}{m_c^2}\frac{(x-y)^2}{x(1-x)y(1-y)(x+y-2xy)^2},\\
T_{H2}^{p\sigma}(x,y,m_c^2) &= \frac{\mathcal{N}_0\alpha_s^2(m_c^2)}{432\sqrt{3}m_c^2}\frac{\mu_\pi^2}{m_c^2}\frac{(8y^2-8y+1)x^2+2y(-4y^2+2y+1)x+y^2(4y-3)}{x(1-x)y^2(1-y)^2(x+y-2xy)^3},\\
T_{H2}^{\sigma p}(x,y,m_c^2) &= \frac{\mathcal{N}_0\alpha_s^2(m_c^2)}{432\sqrt{3}m_c^2}\frac{\mu_\pi^2}{m_c^2}\frac{(4-8y)x^3+(8y^2+4y-3)x^2+2(1-4y)yx+y^2)}{x^2(1-x)^2y(1-y)(x+y-2xy)^3},\\
T_{H2}^{\sigma\sigma}(x,y,m_c^2) &= \frac{\mathcal{N}_0\alpha_s^2(m_c^2)}{2592\sqrt{3}m_c^2}\frac{\mu_\pi^2}{m_c^2}\frac{1}{x^2(1-x)^2y^2(1-y)^2(x+y-2xy)^4}((24y^3-36y^2+14y-1)x^5+(-144y^4+228y^3\\
&\quad-119y^2+30y-3)x^4+(8y^5+268y^4-424y^3+210y^2-46y+3)x^3+y(-12y^4-175y^3+242y^2\\
&\quad-84y+10)x^2+2y^2(3y^3+23y^2-27y+5)x-y^3(y^2+3y-3))
\end{aligned}
\tag{21}
$$

for $J=2$.

III. THE WAVE FUNCTIONS OF LIGHT MESONS

In the above calculation, the twist-2,3 wave functions and distribution amplitudes of pion and kaon are the main nonperturbative input parameters for mHSA and sHSA, respectively. In this section, we will discuss them in detail. According to BHL prescription [12], one can connect the equal-time wave function in the rest frame and the light-cone wave function by equating the off-shell propagator in the two frames. The wave function for quark-antiquark systems at the infinite momentum frame can be got from the harmonic oscillator model at the rest frame

$$
\Psi(x,\mathbf{k}_\perp)\propto\exp\left[-\frac{1}{8\beta^2}\left(\frac{\mathbf{k}_\perp^2+m_1^2}{x}+\frac{\mathbf{k}_\perp^2+m_2^2}{1-x}\right)\right], \tag{22}
$$

where m_i and β are the constitute quark mass and the harmonic parameter, respectively. The distribution amplitude can be obtained from the integration of wave function over the transverse momentum

$$
\phi(x,\mu_F)=\int_{|\mathbf{k}_\perp|<\mu_F}\frac{d^2\mathbf{k}_\perp}{16\pi^3}\Psi(x,\mathbf{k}_\perp), \tag{23}
$$

where μ_F is the ultraviolet cutoff.

Upon expansion over Gegenbauer polynomials, twist-2 wave functions of pion and kaon with the transverse momentum dependence can be characterized as

$$
\begin{aligned}
\Psi_\pi^\pi(x,\mathbf{k}_\perp) &= A_\pi^\pi[1+B_\pi^\pi C_2^{3/2}(2x-1)\\
&\quad+C_\pi^\pi C_4^{3/2}(2x-1)]\exp\left[-\frac{\mathbf{k}_\perp^2+m_q^2}{8\beta_\pi^2x(1-x)}\right]
\end{aligned}
\tag{24}
$$

and

$$\Psi_K^K(x,\mathbf{k}_\perp) = A_K^K[1 + B_K^K C_1^{3/2}(2x-1) + C_K^K C_2^{3/2}(2x-1)]\exp\left[-\frac{1}{8\beta_K^2}\left(\frac{\mathbf{k}_\perp^2 + m_q^2}{x} + \frac{\mathbf{k}_\perp^2 + m_s^2}{1-x}\right)\right], \tag{25}$$

where $C_n^{3/2}$ are Gegenbauer polynomials and q means light quark u or d. For the SU(2) isotopic symmetry, the odd expansion terms do not appear in the pion wave functions. On the contrary, the odd expansion terms are not zero in the Kaon wave functions for SU(3)-flavor symmetry breaking. Estimates of first two Gegenbauer moments for twist-3 distribution amplitudes are more uncertain than that of leading-twist distribution amplitudes. To simplify the following numerical analysis, we take twist-3 wave functions as

$$\begin{aligned}\Psi_p^\pi(x,\mathbf{k}_\perp) &= \frac{A_p^\pi}{x(1-x)}\exp\left[-\frac{\mathbf{k}_\perp^2 + m_q^2}{8\beta_\pi^2 x(1-x)}\right],\\ \Psi_\sigma^\pi(x,\mathbf{k}_\perp) &= A_\sigma^\pi \exp\left[-\frac{\mathbf{k}_\perp^2 + m_q^2}{8\beta_\pi^2 x(1-x)}\right]\end{aligned} \tag{26}$$

and

$$\begin{aligned}\Psi_p^K(x,\mathbf{k}_\perp) &= \frac{A_p^K}{x(1-x)}\exp\left[-\frac{1}{8\beta_K^2}\left(\frac{\mathbf{k}_\perp^2 + m_q^2}{x} + \frac{\mathbf{k}_\perp^2 + m_s^2}{1-x}\right)\right],\\ \Psi_\sigma^K(x,\mathbf{k}_\perp) &= A_\sigma^K \exp\left[-\frac{1}{8\beta_K^2}\left(\frac{\mathbf{k}_\perp^2 + m_q^2}{x} + \frac{\mathbf{k}_\perp^2 + m_s^2}{1-x}\right)\right]\end{aligned} \tag{27}$$

for pion and kaon, respectively.

Substituting Eq. (24)–(27) into Eq. (23), the distribution amplitudes of pion and kaon are written as

$$\phi_\pi^\pi(x) = \frac{A_\pi^\pi \beta_\pi^2}{2\pi^2}x(1-x)[1 + B_\pi^\pi C_2^{3/2}(2x-1) + C_\pi^\pi C_4^{3/2}(2x-1)]\exp\left[-\frac{m_q^2}{8\beta_\pi^2 x(1-x)}\right], \tag{28}$$

$$\phi_K^K(x) = \frac{A_K^K \beta_K^2}{2\pi^2}x(1-x)[1 + B_i^K C_1^{3/2}(2x-1) + C_i^K C_2^{3/2}(2x-1)]\exp\left[-\frac{(1-x)m_q^2 + x m_s^2}{8\beta_K^2 x(1-x)}\right], \tag{29}$$

for twist-2 distribution amplitudes and

$$\begin{aligned}\phi_p^\pi(x) &= \frac{A_p^\pi \beta_\pi^2}{2\pi^2}x(1-x)\exp\left[-\frac{m_q^2}{8\beta_\pi^2 x(1-x)}\right],\\ \phi_\sigma^\pi(x) &= \frac{A_\sigma^\pi \beta_\pi^2}{2\pi^2}\exp\left[-\frac{m_q^2}{8\beta_\pi^2 x(1-x)}\right],\end{aligned} \tag{30}$$

$$\begin{aligned}\phi_p^K(x) &= \frac{A_p^K \beta_K^2}{2\pi^2}\exp\left[-\frac{(1-x)m_q^2 + x m_s^2}{8\beta_K^2 x(1-x)}\right],\\ \phi_\sigma^K(x) &= \frac{A_\sigma^K \beta_K^2}{2\pi^2}x(1-x)\exp\left[-\frac{(1-x)m_q^2 + x m_s^2}{8\beta_K^2 x(1-x)}\right]\end{aligned} \tag{31}$$

for twist-3 distribution amplitudes. With the help of the above distribution amplitudes from BHL prescription, the end point problem can be cured in the standard HSA since the exponential suppression appears in $x = 0$ and $x = 1$ point.

For definiteness, we take the conventional values for the constitute quark masses: $m_q = 0.30$ GeV and $m_s = 0.45$ GeV. The parameters, A_i^j, B_j^j, C_j^j and β_j ($i = \pi, K, p, \sigma$; $j = \pi, K$) can be determined by some constraints on the general properties of the light mesons wave functions. In the pion and kaon case, the harmonic parameters β_π and β_K are obtained by the constraints $\langle\mathbf{k}_\perp^2\rangle_K \approx \langle\mathbf{k}_\perp^2\rangle_\pi \approx (0.356\ \text{GeV})^2$, which are the average values of the transverse momentum square defined as

$$\langle\mathbf{k}_\perp^2\rangle_i = \frac{f_i^2}{24}\int dx\frac{d^2\mathbf{k}_\perp}{16\pi^3}|\mathbf{k}_\perp^2||\Psi_i(x,\mathbf{k}_\perp)|^2/P_{q\bar{q}}^i \tag{32}$$

with $i = \pi, K$ and Ψ_i stand for twist-2 wave functions Ψ_π^π and Ψ_K^K. The decay constants are taken as $f_\pi = 0.132$ GeV for the pion and $f_K = 0.160 GeV$ for the kaon. The probability of finding the $q\bar{q}$ leading-twist Fock state in a pion or kaon should be not larger than unity,

$$P_{q\bar{q}}^i = \frac{f_i^2}{24}\int dx\frac{d^2\mathbf{k}_\perp}{16\pi^3}|\Psi_i(x,\mathbf{k}_\perp)|^2 \le 1. \tag{33}$$

The others coefficients are extracted by the normalization condition

$$\int dx\frac{d^2\mathbf{k}_\perp}{16\pi^3}\Psi_i^j(x,\mathbf{k}_\perp) = 1 \tag{34}$$

with ($i = \pi, K, p, \sigma$; $j = \pi, K$) and first two Gegenbauer moments of twist-2 distribution amplitudes a_i^j ($i = 2, 4$ for $j = \pi$; $i = 1, 2$ for $j = K$.). The coefficients a_i^j at some reference scale μ_F are nonperturbative quantities and have to be evaluated using a nonperturbative technique or must be extracted from experiment. It turns out that the determination of a_2^π receives large errors, whether by direct calculations using QCD sum rules [20] or by analysis of experimental data on the pion electromagnetic and transition form factors [21]. Totally, the averages of the second moment are probably

$$a_2^{\pi}(1\ \text{GeV}) = 0.25 \pm 0.15,$$
$$a_2^{K}(1\ \text{GeV}) = 0.25 \pm 0.15, \quad (35)$$

in Ref. [14], including radiative corrections to the sum rules.

The numerical value of the first moment a_1^K was the subject of significant controversy until recently. The existing estimates are all obtained using different versions of QCD sum rules [22–25] and yield an average [14]

$$a_1^K(1\ \text{GeV}) = 0.06 \pm 0.03. \quad (36)$$

Estimates of yet higher-order Gegenbauer moments are rather uncertain. The fourth Gegenbauer moment of the pion twist-2 distribution amplitude [26] was constrained

$$a_4^{\pi}(1\ \text{GeV}) = 0.04 \pm 0.11, \quad (37)$$

which is consistent with the results from the light-cone sum rule calculations of the transition form factor $F_{\pi\gamma\gamma^*}$ in Refs. [27–29].

According to QCD evolution of the wave function, the coefficients a_i^j at a factorization scale μ_F can be expressed as $a_i^j(\mu_F^2) = a_i^j(\mu_0^2)(\alpha_s(\mu_F^2)/\alpha_s(\mu_0^2))^{\gamma_i}$. $a_i^j(\mu_0^2)$ are a nonperturbative coefficients, μ_0 is a typical hadronic scale, $0.5 \leq \mu_0 \leq 1$ GeV, and γ_i are the anomalous dimensions. In this work, a reasonable factorization scale should be chosen as $\mu_F = m_c$, $1.35 \leq m_c \leq 1.8$ GeV. The values of the coefficients a_i^j at $\mu_F = 1$ GeV and $\mu_F = 2$ GeV are listed in Table III of Ref. [14]. For example, $a_1^K(1\ \text{GeV}) = 0.06 \pm 0.03$ and $a_1^K(2\ \text{GeV}) = 0.05 \pm 0.02$. By analyzing these data, we find that it is feasible to choose Gegenbauer moments a_i^j at $\mu_F = 1$ GeV in our calculation.

Taking account of the above Gegenbauer moments for the pion and kaon twist-2 distribution amplitudes, we figure out harmonic parameters $\beta_{\pi,K}$, probabilities of finding the $q\bar{q}$ leading-twist Fock state $P_{q\bar{q}}^{\pi,K}$ and Gegenbauer coefficients A_i^j, B_j^j, C_j^j ($i = \pi, K, p, \sigma$; $j = \pi, K$). Those values are list in Table II. According to uncertainties of twist-2 Gegenbauer moments, the parameters of the pion and kaon are given in three parts: upper limit, central value and lower limit. Since $P_{q\bar{q}}^{\pi} \leq 0.270$ and $P_{q\bar{q}}^{K} \leq 0.492$ are much smaller than unity, higher twist and higher Fock states are important components of the pion and kaon.

TABLE II. The parameters of twist-2,3 wave functions for the pion and kaon mesons in Eqs. (24)–(31). The dimensions of harmonic parameters $\beta_{\pi,K}$ and normalization coefficients A_i^j ($i = \pi, K, p, \sigma$; $j = \pi, K$.) are GeV and $(\text{GeV})^{-2}$, respectively. The others parameters is dimensionless.

π	β_π	$P_{q\bar{q}}^{\pi}$	A_π^π	B_π^π	C_π^π	A_p^π	A_σ^π
upper limit	0.512	0.270	672.28	0.628	0.354	106.92	574.47
central value	0.461	0.249	849.18	0.469	0.213	140.88	747.55
lower limit	0.418	0.259	1034.30	0.259	0.023	184.29	965.85
K	β_K	$P_{q\bar{q}}^{K}$	A_K^K	B_K^K	C_K^K	A_p^K	A_σ^K
upper limit	0.461	0.492	1108.83	0.253	0.618	170.59	883.49
central value	0.442	0.422	1196.66	0.215	0.477	193.81	998.32
lower limit	0.417	0.398	1353.56	0.175	0.323	232.44	1188.23

In the mHSA, the convolutions of wave functions and hard- scattering amplitudes are presented in transverse configuration b-space. We need to define wave function in b-space by Fourier transformation

$$\Psi^i(x, \mathbf{b}) = \int \frac{d^2\mathbf{k}_\perp}{(2\pi)^2} \Psi^i(x, \mathbf{k}_\perp) e^{-i\mathbf{k}_\perp \cdot \mathbf{b}}$$
$$= 4\pi\phi^i(x) \exp[-2\beta_i^2 x(1-x) b^2], \quad (38)$$

where Ψ^i and ϕ^i stand for wave function Ψ_j^i and distribution amplitude ϕ_j^i ($i = \pi, K, p, \sigma$; $j = \pi, K$), respectively. One may observe that wave functions in the b-space are also highly suppressed in the end-point region. Such feature is necessary to suppress the end-point singularity coming from the hard-scattering amplitudes and then to derive a more reasonable results.

IV. NUMERICAL ANALYSIS

In our calculations for the decay ratio of χ_{cJ} to light pseudoscalar pairs, the partial of P-wave function at the origin $R_p'(0)$ is also an important nonperturbative input parameter. It is shown that this parameter is a function of the charm-quark mass m_c both in the well-know quarkonium potential models [33,34] and in the global fit of charmonium parameters [35]. To obtain its expression relative to the charm-quark mass, which is consisted with our approach, the decay width of the χ_{c0} annihilating into two photons need to be calculated by the same approach. With the help of Refs. [35–38], we obtain

$$\Gamma[\chi_{c0} \to \gamma\gamma] = 27 Q_c^4 \alpha_{\text{em}}^2 \frac{|R_p'(0)|^2}{m_c^4} \left[1 + \left(\frac{\pi^2}{3} - \frac{28}{9}\right) \frac{\alpha_s(m_c^2)}{\pi}\right], \quad (39)$$

where the one-loop QCD radiative correction is included, $Q_c = \frac{2}{3}$ is the charge of the c-quark and $\alpha_{\text{em}} = \frac{1}{137}$ is the electromagnetic coupling constant.

The running coupling constant $\alpha_s(Q^2)$ up to next-to-leading-log is written as

$$\frac{\alpha_s(Q^2)}{\pi} = \frac{1}{\beta_1 \ln(Q^2/\Lambda_{\text{QCD}}^2)} - \frac{\beta_2}{\beta_1^3} \frac{\ln\ln(Q^2/\Lambda_{\text{QCD}}^2)}{\ln^2(Q^2/\Lambda_{\text{QCD}}^2)} \quad (40)$$

with $\beta_1 = (33 - 2n_f)/12$ and $\beta_2 = (153 - 19n_f)/24$. Here we take quark-flavor number $n_f = 4$ and the QCD scale $\Lambda_{\text{QCD}} = 0.25$ GeV.

The decay width of the χ_{c0} annihilating into two photons can be obtained from Refs. [30,39]. Using the above data and formulas, the relation between $R_p'(0)$ and m_c is shown in Fig. 2 with uncertainty of the χ_{c0} two-photon decay width. The solid curve comes from taking central-value

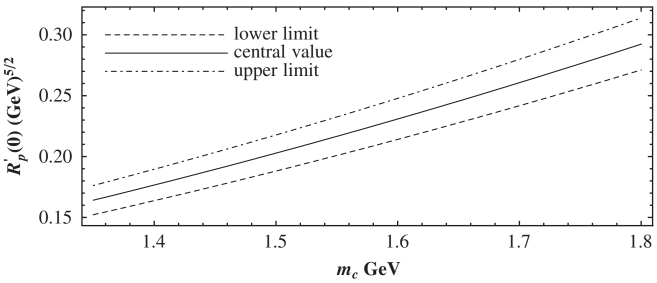

FIG. 2. Dependence of the partial of P-wave function at the origin $R_p'(0)$ for P-wave charmonium on the c-quark mass m_c with uncertainty of the χ_{c0} two-photon decay width.

$\Gamma[\chi_{c0} \to \gamma\gamma] = 2.37$ keV. The dot-dashed and dashed curves are given by taking upper limit $\Gamma[\chi_{c0} \to \gamma\gamma] = 2.71$ keV and lower limit $\Gamma[\chi_{c0} \to \gamma\gamma] = 2.03$ keV, respectively. We find that uncertainty with different χ_{c0} two-photon decay width is less than 10%. So we will take the result of the central value in the following. The region of the charm-quark mass is $m_c = 1.35$–1.8 GeV from Ref. [4]. Comparing our $R_p'(0)$ with values of Ref. [4], there are some differences that our value is less than one of Ref. [4] as $m_c = 1.35$ GeV and vice versa as $m_c = 1.8$ GeV.

On the other hand, the chiral enhancing scales μ_π and μ_K, which are scales characterized by the chiral perturba-

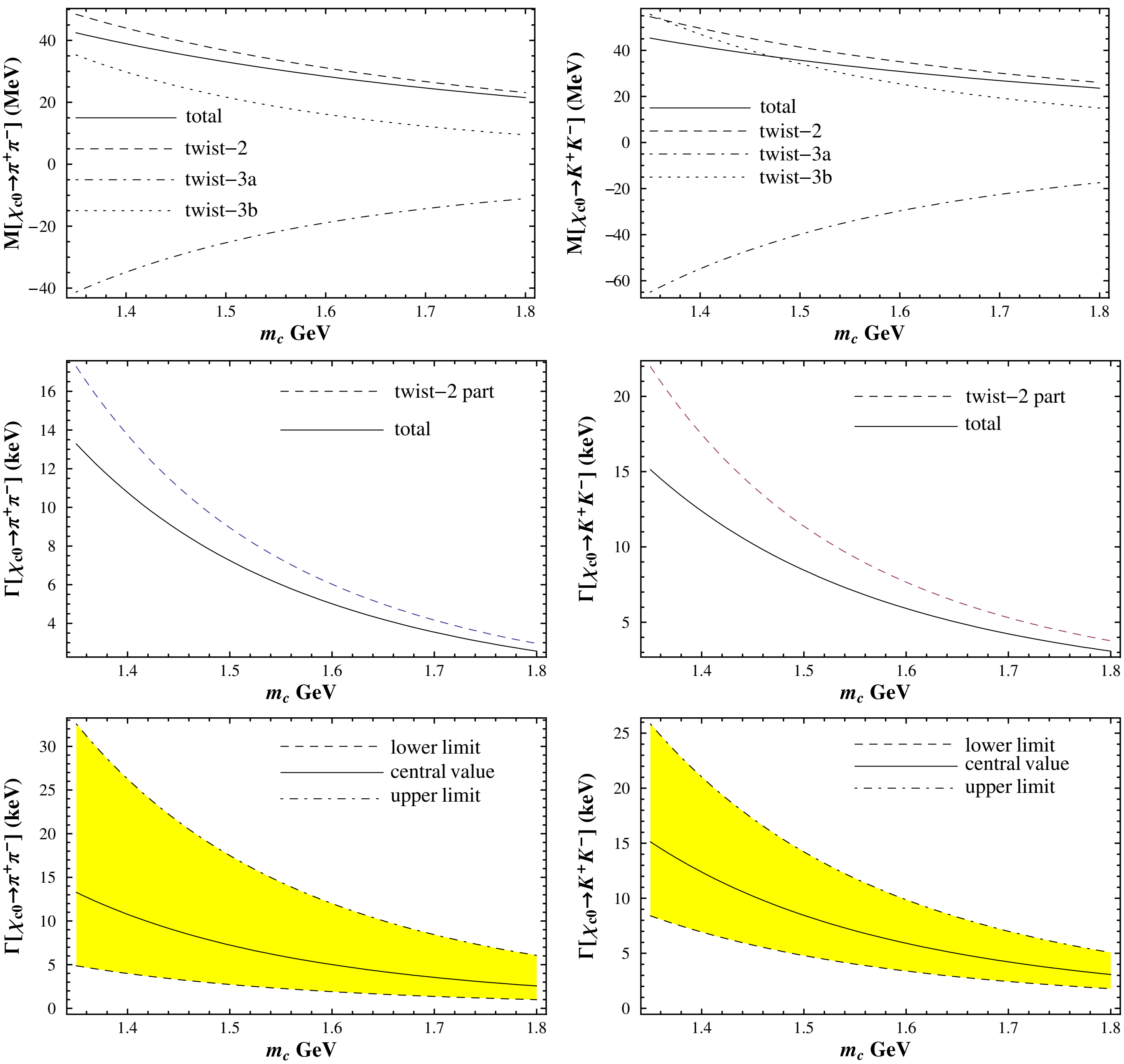

FIG. 3 (color online). Dependence of the prediction for the $\chi_{c0} \to \pi^+\pi^-$ and K^+K^- decay widths on the c-quark mass m_c with contribution from twist-3 distribution amplitudes of the pion and kaon meson in sHSA, respectively.

tion theory, are important parameters which can affect contributions from twist-3 parts sensitively. However, they are difficult to give precise numbers as long as the current quark masses are not more accurately known. To obtain reasonable numerical analysis with acceptable estimates for the chiral enhancing scales, we take $\mu_\pi(1\ \text{GeV}) = 1.5\ \text{GeV}$ and $\mu_K(1\ \text{GeV}) = 1.7\ \text{GeV}$, which are consistent with the results from pQCD application [40,41] and chiral perturbation theory [42].

In the above discussion, nonperturbative input parameters appearing in our calculation are obtained by a model wave function or distribution amplitude, a fit experimental data and a reasonable evaluation. Next, we will do numerical analysis for the charmonium $\chi_{c0,2}$ decay rates into two pions or two kaons with the charge case in the sHSA and in the mHSA, respectively.

The decay widths of $\chi_{cJ} \to \pi^+\pi^-$ and K^+K^- ($J = 0, 2$) by the sHSA are shown in Figs. 3 and 4 with the

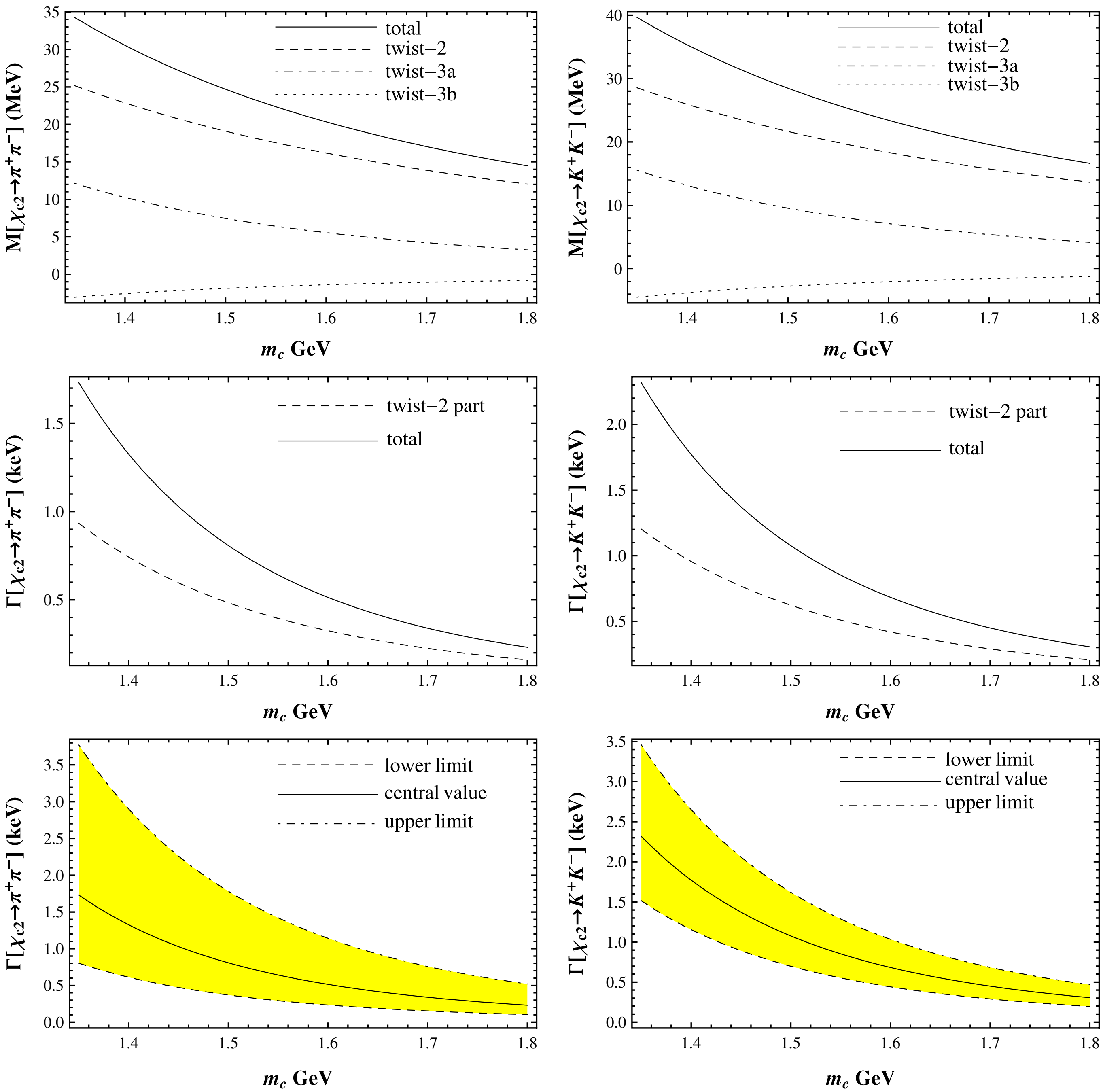

FIG. 4 (color online). Dependence of the prediction for the $\chi_{c2} \to \pi^+\pi^-$ and K^+K^- decay widths on the c-quark mass m_c with contribution from twist-3 distribution amplitudes of the pion and kaon meson in sHSA, respectively.

TABLE III. The decay widths for $\chi_{cJ} \to \pi^+\pi^-$ and K^+K^- ($J = 0, 2$) from experimental data. The BES results are evaluated with the BES result for the total width. In the other cases the PDG average values for the total widths are used.

	PDG [30]	BES [31]	Belle [32]
$\Gamma[\chi_{c0} \to \pi^+\pi^-]$ [kev]	50 ± 8	67 ± 36	60 ± 21
$\Gamma[\chi_{c0} \to K^+K^-]$ [kev]	60 ± 10	81 ± 45	57 ± 19
$\Gamma[\chi_{c2} \to \pi^+\pi^-]$ [kev]	2.8 ± 0.5	3.0 ± 1.0	3.4 ± 1.3
$\Gamma[\chi_{c2} \to K^+K^-]$ [kev]	1.5 ± 0.4	1.6 ± 0.7	2 ± 0.9

c-quark mass m_c as a variable parameter. We take the central-value of Table II as the input parameters for the top two and middle two figures. The top two figures are the decay amplitudes for two-pion and two-kaon decays, where the dashed curve is the contribution from twist-2 part, the dotted and dot-dashed are contributions from twist-3 parts named a and b and the solid curve is the sum. The twist-3a is the positive and the twist-3b is the negative which are corresponding to the positive and negative terms in Eq. (20) and (21).

The large enhancement of the total amplitudes in the χ_2 channel indicates that the twist-3 distribution amplitudes play important pole. The results for the decay width are shown in the middle two figures of Fig. 4 where the solid curve is the total decay width and the dashed curve is the for twist-2 part. In the χ_0 channel, the corrections are not so large since the two contributions from twist-3a and b parts have opposite sign and have large cancellation. The results with the uncertainty of twist-2 distribution amplitude are shown in the bottom two figures, where the solid curve is for the central value, the dashed and dot-dashed curve are for lower limit and upper limit, respectively. We can see the uncertain is very large which shows the sensitivity on the distribution amplitude.

Comparing the results with experimental data [30–32], which are list in Table III, we see that the decay widths of χ_0 channel are smaller than experimental data for all variable m_c and the decay widths of the χ_2 channel are in agreement with the experimental data in the region $m_c <$ 1.5 GeV.

In Fig. 5, we show the curves of the widths of the $\chi_{c0,2}$ into two pions or two kaons on the c-quark mass m_c by the mHSA method. The solid curve is the decay width where only the twist-2 contribution is considered and the parameters are taken as the central values. The shadow is the total decay width where the uncertainty of twist-2 Gegenbauer moments are considered. Here we see that the shade region

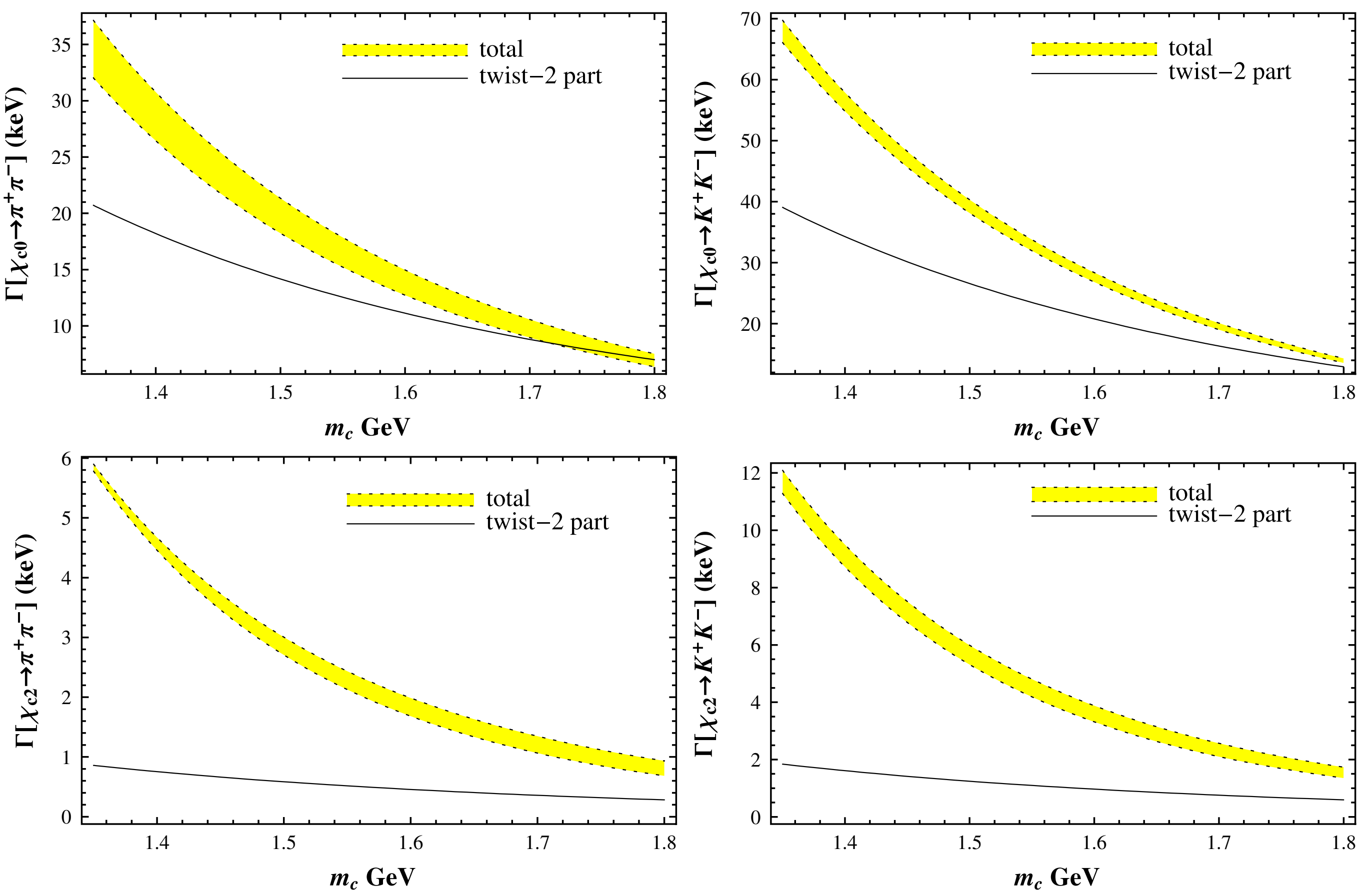

FIG. 5 (color online). Dependence of the prediction for the $\chi_{cJ} \to \pi^+\pi^-$ and K^+K^- ($J = 0, 2$) decay widths on the c-quark mass m_c with contribution from twist-3 distribution amplitudes of the pion and kaon meson in mHSA, respectively.

is very narrow which means the unsensitivity on the twist-2 distribution amplitude of the light mesons. The decay widths including twist-3 corrections are improved remarkably. Detailedly, the predictions for the decay widths of $\chi_2 \to \pi^+\pi^-$ and $\chi_0 \to K^+K^-$ are comparable with experimental data in the region $m_c \in (1.4, 1.6)$ GeV and $m_c \in (1.35, 1.6)$ GeV, respectively. This is very different with the sHSA method which suggests the necessary of the mHSA method.

V. CONCLUSION

In this paper, we presented a detailed analysis of $\chi_{c0,2}$ decays into two pions and two kaons including the twist-3 contribution within the framework of the sHSA and mHSA methods. In the sHSA, the end-point problem is overcome by using BHL prescription where a exponential suppression is introduced in the expression of hadronic wave functions or distribution amplitudes. The uncertainty of the results on the twist-2 Gegenbauer moments for the pion and kaon is analyzed and is rather small in the mHSA method. The results indicate the larger contributions from twist-3 distribution amplitude which have not been analyzed before. And both the decay widths of $\chi_{c0,2}$ to $\pi^+\pi^-$ and K^+K^- are found to be comparable with the experimental data in the region $m_c \in (1.35, 1.8)$ GeV when including twist-3 correction in the mHSA.

ACKNOWLEDGMENTS

This work was supported partially by the Natural Science Foundation of China, Grant Number: 10747154, 10805009 and 10575083.

APPENDIX A: THE COEFFICIENTS OF HARD-SCATTERING AMPLITUDES

In this Appendix we present the explicit expression of the coefficients $C_i^I(J)(I = pp, p\sigma, \sigma p, \sigma\sigma)$ appearing in the Eq. (14) for hard-scattering amplitudes.

$$C_1^{pp}(0) = 5, \qquad C_0^{pp}(0) = 2m_c^2(x^2 + 2(y-1)x + (y-2)y), \tag{A1}$$

$$C_1^{pp}(2) = 2, \qquad C_0^{pp}(2) = -4m_c^2(x^2 - 4yx + x + y^2 + y) \tag{A2}$$

for hard-scattering amplitude $T_{HJ}^{pp}(x, y, \mathbf{k}_1, \mathbf{k}_2)$ with $J = 0, 2$.

$$\begin{aligned} &C_3^{p\sigma}(0) = 5m_c^2, \qquad C_2^{p\sigma}(0) = 4m_c^4(4x^2 + (4y-6)x - 2y - 3),\\ &C_1^{p\sigma}(0) = -4m_c^6(11x^2 + 2(7y-9)x + y(3y-10)),\\ &C_0^{p\sigma}(0) = -16m_c^8(2x^4 + (6y-7)x^3 + 3(2y^2 - 5y + 2)x^2 + y(2y^2 - 9y + 8)x - (y-2)y^2) \end{aligned} \tag{A3}$$

and

$$\begin{gathered} C_3^{p\sigma}(2) = 8m_c^2, \qquad C_2^{p\sigma}(2) = -8m_c^4(4x^2 - 8yx + 4y + 3), \qquad C_1^{p\sigma}(2) = 16m_c^6(4x^2 + (3 - 14y)x + 7y),\\ C_0^{p\sigma}(2) = 64m_c^8(x^4 - 2x^3 - 3(y-1)yx^2 - 2y(y^2 - 3y + 1)x + (y-2)y^2) \end{gathered} \tag{A4}$$

for hard-scattering amplitude $T_{HJ}^{p\sigma}(x, y, \mathbf{k}_1, \mathbf{k}_2)$ with $J = 0, 2$.

$$\begin{aligned} &C_3^{\sigma p}(0) = 5m_c^2, \qquad C_2^{\sigma p}(0) = 4m_c^4(4y^2 - 6y + x(4y-2) - 3),\\ &C_1^{\sigma p}(0) = -4m_c^6(3x^2 + 2(7y-5)x + y(11y-18)),\\ &C_0^{\sigma p}(0) = -16m_c^8((2y-1)x^3 + (6y^2 - 9y + 2)x^2 + y(6y^2 - 15y + 8)x + y^2(2y^2 - 7y + 6)) \end{aligned} \tag{A5}$$

and

$$\begin{gathered} C_3^{\sigma p}(2) = 8m_c^2, \qquad C_2^{\sigma p}(2) = -8m_c^4(4y^2 + x(4 - 8y) + 3), \qquad C_1^{\sigma p}(2) = 16m_c^6(x(7 - 14y) + y(4y + 3)),\\ C_0^{\sigma p}(2) = -64m_c^8((2y-1)x^3 + (3y^2 - 6y + 2)x^2 + (2 - 3y)yx - (y-2)y^3) \end{gathered} \tag{A6}$$

for hard-scattering amplitude $T_{HJ}^{\sigma p}(x, y, \mathbf{k}_1, \mathbf{k}_2)$ with $J = 0, 2$.

$$
\begin{aligned}
C_6^{\sigma\sigma}(0) &= 7m_c^2, \qquad C_5^{\sigma\sigma}(0) = -2m_c^4(7x^2 - 7x + 11y^2 - 11y + 39),\\
C_4^{\sigma\sigma}(0) &= 2m_c^6((26 - 52y)x^3 + (-104y^2 + 182y - 101)x^2 - 2(26y^3 - 91y^2 + 173y - 85)x + 26y^3 - 69y^2 + 138y + 40),\\
C_3^{\sigma\sigma}(0) &= -16m_c^8(x^4 + (8y - 6)x^3 + 2(5y^2 - 11y - 3)x^2 - 2(5y^2 + 18y - 18)x - 3y^4 + 6y^3 - 6y^2 + 28y - 6),\\
C_2^{\sigma\sigma}(0) &= 32m_c^{10}((8y - 4)x^5 + 4(8y^2 - 13y + 5)x^4 + 2(24y^3 - 68y^2 + 62y - 19)x^3\\
&\quad + (32y^4 - 136y^3 + 200y^2 - 130y + 35)x^2 + 2(4y^5 - 26y^4 + 54y^3 - 53y^2 + 31y - 9)x\\
&\quad + y(-4y^4 + 12y^3 - 14y^2 + 19y - 18)),\\
C_1^{\sigma\sigma}(0) &= 32m_c^{12}(x^6 + (1 - 8y)x^5 + (-45y^2 + 65y - 9)x^4 - 2(40y^3 - 105y^2 + 50y + 6)x^3\\
&\quad + (-65y^4 + 250y^3 - 214y^2 - 36y + 36)x^2 + y(-24y^4 + 125y^3 - 164y^2 - 20y + 72)x\\
&\quad + y^2(-3y^4 + 21y^3 - 41y^2 + 4y + 36)),\\
C_0^{\sigma\sigma}(0) &= -96m_c^{14}(x^2 + 2(y - 1)x + (y - 2)y)^3(-2y + x(4y - 2) - 1)
\end{aligned}
\tag{A7}
$$

and

$$
\begin{aligned}
C_6^{\sigma\sigma}(2) &= 4m_c^2, \qquad C_5^{\sigma\sigma}(2) = 4m_c^4(7x^2 - (12y + 1)x + 11y^2 - 5y - 6),\\
C_4^{\sigma\sigma}(2) &= 4m_c^6(26(2y - 1)x^3 + (-208y^2 + 130y - 61)x^2 + (52y^3 + 130y^2 - 32y + 25)x - 26y^3 - 93y^2 + 57y - 4),\\
C_3^{\sigma\sigma}(2) &= 32m_c^8(x^4 + (21 - 46y)x^3 + (118y^2 - 49y + 15)x^2 - y(54y^2 + 37y + 6)x - 3y^4 + 33y^3 + 15y^2 - 8y + 6),\\
C_2^{\sigma\sigma}(2) &= -32m_c^{10}(8(2y - 1)x^5 + (-32y^2 - 8y + 7)x^4 + (-96y^3 + 208y^2 - 166y + 53)x^3 + (-32y^4 + 208y^3 - 26y^2\\
&\quad - 29y + 10)x^2 + (16y^5 - 8y^4 - 198y^3 + 19y^2 - 56y + 30)x + y(-8y^4 - 9y^3 + 101y^2 - 22y + 30)),\\
C_1^{\sigma\sigma}(2) &= -64m_c^{12}(x^6 + (13 - 32y)x^5 + (51y^2 + 29y - 12)x^4 + 2(80y^3 - 171y^2 + 64y - 12)x^3 + (31y^4 - 302y^3\\
&\quad + 248y^2 + 24y - 24)x^2 + y(-48y^4 + 89y^3 + 64y^2 + 40y - 48)x - y^2(3y^4 - 33y^3 + 44y^2 + 8y + 24)),\\
C_0^{\sigma\sigma}(2) &= 192m_c^{14}(x^2 + 2(y - 1)x + (y - 2)y)^2((4y - 2)x^3 + (-16y^2 + 10y - 3)x^2\\
&\quad + (4y^3 + 10y^2 - 1)x - y(2y^2 + 3y + 1))
\end{aligned}
\tag{A8}
$$

for hard-scattering amplitude $T_{HJ}^{\sigma p}(x, y, \mathbf{k}_1, \mathbf{k}_2)$ with $J = 0, 2$.

APPENDIX B: THE COEFFICIENTS OF THE FOURIER TRANSFORM

In this appendix we present the explicit expression of the coefficients $A_{1i}^I(J)$, $A_{2i}^I(J)$ and $B_i^I(J)$ appearing in the Eq. (16) for the Fourier transform of hard-scattering amplitude. First, we show some useful formulas for Fourier transform,

$$
\int \frac{d^2\mathbf{k}}{(2\pi)^2}\frac{e^{-i\mathbf{k}\cdot\mathbf{b}}}{(s - \mathbf{k}^2 + i\epsilon)^n} = \frac{(-)^n}{(n-1)!}\begin{cases}\frac{i}{4}\frac{d^{n-1}}{ds^{n-1}}[H_0^{(1)}(\sqrt{s}b)] & \text{for } s > 0\\ \frac{1}{2\pi}\frac{d^{n-1}}{ds^{n-1}}[K_0(\sqrt{-s}b)] & \text{for } s < 0\end{cases}
\tag{B1}
$$

with $n = 1, 2, \cdots$.

The coefficients $A_{1i}^I(J)$, $A_{2i}^I(J)$ and $B_i^I(J)$, coming from the Fourier transform of hard-scattering amplitudes, are given as,

$$
\begin{aligned}
A_{10}^{\pi\pi}(J) &= \frac{2(x + y) + (-2)^{J/2}(x - y)^2}{8(x + y - 1)(x + y)^2}, \qquad A_{20}^{\pi\pi}(J) = \frac{2(2 - x - y) + (-2)^{J/2}(x - y)^2}{8(x + y - 1)(2 - x - y)^2},\\
B_0^{\pi\pi}(J) &= \frac{(x + y)(2 - x - y) + (-2)^{J/2}(x - y)^2}{\pi(x + y)^2(2 - x - y)^2}, \qquad B_1^{\pi\pi}(J) = \frac{(-2)^{J/2}b(x - y)^2}{4\sqrt{2}\pi(x + y)(2 - x - y)\sqrt{x + y - 2xy}}
\end{aligned}
\tag{B2}
$$

with $b = 2m_cb_1$ for $\mathcal{T}_{HJ}^{\pi\pi}(x, y, \mathbf{b}_1, \mathbf{b}_2)$,

$$A_{10}^{pp}(0) = \frac{x+y+3}{4(x+y-1)(x+y)}, \qquad A_{20}^{pp}(0) = \frac{5-x-y}{4(x+y-1)(2-x-y)},$$
$$B_0^{pp}(0) = \frac{3}{\pi(x+y)(2-x-y)}, \qquad B_1^{pp}(0) = -\frac{b}{2\sqrt{2}\pi\sqrt{x+y-2xy}} \tag{B3}$$

for $\mathcal{T}_{H0}^{pp}(x, y, \mathbf{b}_1, \mathbf{b}_2)$,

$$A_{10}^{pp}(2) = \frac{4xy-x^2-y^2}{2(x+y-1)(x+y)^2}, \qquad A_{20}^{pp}(2) = \frac{4(1-x)(1-y)-(1-x)^2-(1-y)^2}{2(x+y-1)(2-x-y)^2},$$
$$B_0^{pp}(2) = \frac{-6(x-y)^2}{\pi(x+y)^2(2-x-y)^2}, \qquad B_1^{pp}(2) = \frac{-b((x-y)^2+x+y-2xy)}{\sqrt{2}\pi(x+y)(2-x-y)\sqrt{x+y-2xy}} \tag{B4}$$

for $\mathcal{T}_{H2}^{pp}(x, y, \mathbf{b}_1, \mathbf{b}_2)$,

$$A_{10}^{p\sigma}(0) = -\frac{4x^2+(2y-3)x-2y^2+y}{8(x+y-1)^2(x+y)^3}, \qquad A_{20}^{p\sigma}(0) = \frac{4x^2+(2y-7)x-2y^2+y+2}{8(x+y-1)^2(2-x-y)^3},$$
$$A_{11}^{p\sigma}(0) = \frac{-bx}{16(x+y-1)(x+y)\sqrt{xy}}, \qquad A_{21}^{p\sigma}(0) = \frac{-b(1-x)}{16(x+y-1)(2-x-y)\sqrt{(1-x)(1-y)}}$$
$$\begin{aligned}B_0^{p\sigma}(0) = {}& \frac{1}{32\pi(x+y)^3(2-x-y)^3(x+y-2xy)}(2b^2x^6+b^2(10y-11)x^5+5b^2(4y^2-9y+4)x^4\\ &+2((10y^3-35y^2+32y-6)b^2-160y+80)x^3+2(5b^2y^4-25b^2y^3+4(9b^2-16)y^2\\ &+(304-14b^2)y-96)x^2+y(2b^2y^4-15b^2y^3+32(b^2+6)y^2-20(b^2+8)y-128)x\\ &-y^2(b^2y^3-4b^2y^2+4(b^2+24)y-64))\end{aligned}$$
$$B_1^{p\sigma}(0) = \frac{b(2x^4+(26y-17)x^3+(14y^2-53y+18)x^2+y(-10y^2+y+16)x+y^2(5y-2))}{8\sqrt{2}\pi(2-x-y)^2(x+y)^2\sqrt{x+y-2xy}(2xy-x-y)}$$
$$B_2^{p\sigma}(0) = \frac{b^2(2x^2+(2y-3)x-y)}{32\pi(x+y)(2-x-y)(x+y-2xy)} \tag{B5}$$

for $\mathcal{T}_{H0}^{p\sigma}(x, y, \mathbf{b}_1, \mathbf{b}_2)$,

$$A_{10}^{p\sigma}(2) = \frac{4x^2+(2y-3)x-2y^2+y}{4(x+y-1)^2(x+y)^3}, \qquad A_{20}^{p\sigma}(2) = -\frac{4x^2+(2y-7)x-2y^2+y+2}{4(x+y-1)^2(2-x-y)^3},$$
$$A_{11}^{p\sigma}(2) = \frac{bx(x-2y)}{8(x+y-1)(x+y)^2\sqrt{xy}}, \qquad A_{21}^{p\sigma}(2) = \frac{b(x-1)(x-2y+1)}{8(x+y-1)(2-x-y)^2\sqrt{(1-x)(1-y)}}$$
$$\begin{aligned}B_0^{p\sigma}(2) = {}& \frac{1}{8\pi(x+y)^3(2-x-y)^3(x+y-2xy)}(-b^2x^6-2b^2(y-2)x^5+b^2(2y^2+3y-4)x^4\\ &+4(2b^2y^3-4b^2y^2+(b^2+40)y-20)x^3+(7b^2y^4-26b^2y^3+8(3b^2+8)y^2-4(b^2+76)y+96)x^2\\ &+2y(b^2y^4-6b^2y^3+2(5b^2-24)y^2-4(b^2-10)y+32)x-y^2(b^2y^3-4b^2y^2+4(b^2-12)y+32))\end{aligned}$$
$$B_1^{p\sigma}(2) = \frac{-b(x^4+2(8y-5)x^3+(-11y^2-13y+6)x^2-2y(y^2-7y-1)x+(y-4)y^2)}{2\sqrt{2}\pi(2-x-y)^2(x+y)^2\sqrt{x+y-2xy}(2xy-x-y)}$$
$$B_2^{p\sigma}(2) = \frac{-b^2(x^2-2xy+y)}{8\pi(x+y)(2-x-y)(x+y-2xy)} \tag{B6}$$

for $\mathcal{T}_{H2}^{p\sigma}(x, y, \mathbf{b}_1, \mathbf{b}_2)$,

$$A_{10}^{\sigma p}(0) = \frac{2x^2 - (2y+1)x + (3-4y)y}{8(x+y-1)^2(x+y)^3}, \qquad A_{20}^{\sigma p}(0) = \frac{-2x^2 + 2yx + x + 4y^2 - 7y + 2}{8(x+y-1)^2(2-x-y)^3},$$

$$A_{11}^{\sigma p}(0) = \frac{-by}{16(x+y-1)(x+y)\sqrt{xy}}, \qquad A_{21}^{\sigma p}(0) = \frac{-b(1-y)}{16(x+y-1)(2-x-y)\sqrt{(1-x)(1-y)}}$$

$$B_0^{\sigma p}(0) = \frac{1}{32\pi(x+y)^3(2-x-y)^3(x+y-2xy)}(b^2(2y-1)x^5 + b^2(10y^2-15y+4)x^4 + 2((10y^3-25y^2+16y-2)b^2 + 96y - 48)x^3 + 2(10b^2y^4 - 35b^2y^3 + 4(9b^2-16)y^2 - 10(b^2+8)y + 32)x^2 + y(10b^2y^4 - 45b^2y^3 + 64(b^2-5)y^2 + (608-28b^2)y - 128)x + y^2(2b^2y^4 - 11b^2y^3 + 20b^2y^2 - 4(3b^2-40)y - 192))$$

$$B_1^{\sigma p}(0) = \frac{b((5-10y)x^3 + (14y^2+y-2)x^2 + y(26y^2-53y+16)x + y^2(2y^2-17y+18))}{8\sqrt{2}\pi(2-x-y)^2(x+y)^2\sqrt{x+y-2xy}(2xy-x-y)}$$

$$B_2^{\sigma p}(0) = \frac{b^2(y(2y-3) + x(2y-1))}{32\pi(x+y)(2-x-y)(x+y-2xy)} \tag{B7}$$

for $\mathcal{T}_{H0}^{\sigma p}(x, y, \mathbf{b}_1, \mathbf{b}_2)$,

$$A_{10}^{\sigma p}(2) = \frac{-2x^2 + 2yx + x + y(4y-3)}{4(x+y-1)^2(x+y)^3}, \qquad A_{20}^{\sigma p}(2) = -\frac{-2x^2 + 2yx + x + 4y^2 - 7y + 2}{4(x+y-1)^2(2-x-y)^3},$$

$$A_{11}^{\sigma p}(2) = \frac{by(y-2x)}{8(x+y-1)(x+y)^2\sqrt{xy}}, \qquad A_{21}^{\sigma p}(2) = \frac{b(y-1)(y-2x+1)}{8(x+y-1)(2-x-y)^2\sqrt{(1-x)(1-y)}}$$

$$B_0^{\sigma p}(2) = \frac{1}{8\pi(x+y)^3(2-x-y)^3(x+y-2xy)}(b^2(2y-1)x^5 + b^2(7y^2-12y+4)x^4 + ((8y^3-26y^2+20y-4)b^2 - 96y + 48)x^3 + 2(b^2y^4 - 8b^2y^3 + 4(3b^2+8)y^2 - 4(b^2-10)y - 16)x^2 + y(-2b^2y^4 + 3b^2y^3 + 4(b^2+40)y^2 - 4(b^2+76)y + 64)x - y^2(b^2y^4 - 4b^2y^3 + 4b^2y^2 + 80y - 96))$$

$$B_1^{\sigma p}(2) = \frac{b((2y-1)x^3 + (11y^2-14y+4)x^2 + y(-16y^2+13y-2)x - y^2(y^2-10y+6))}{2\sqrt{2}\pi(2-x-y)^2(x+y)^2\sqrt{x+y-2xy}(2xy-x-y)}$$

$$B_2^{\sigma p}(2) = \frac{-b^2(y^2-2xy+x)}{8\pi(x+y)(2-x-y)(x+y-2xy)} \tag{B8}$$

for $\mathcal{T}_{H2}^{\sigma p}(x, y, \mathbf{b}_1, \mathbf{b}_2)$,

$$A_{10}^{\sigma\sigma}(0) = \frac{1}{128(x+-1)^3(x+y)^4}(b^2x^6 + ((6y-1)b^2 - 96y + 64)x^5 + (b^2(15y^2 - 5y - 1) - 8(48y^2 - 36y + 1))x^4 + (b^2(20y^3 - 10y^2 - 4y + 1) - 48(12y^3 - 10y^2 + 4y + 1))x^3 + (3(5b^2 - 128)y^4 + (352 - 10b^2)y^3 - 2(3b^2 + 88)y^2 + 3(b^2 + 48)y + 24)x^2 + y(6(b^2 - 16)y^4 + (96 - 5b^2)y^3 - 4(b^2 - 48)y^2 + 3(b^2 - 16)y - 80)x + y^2(b^2y^4 - b^2y^3 - (b^2 - 184)y^2 + (b^2 - 240)y + 88))$$

$$A_{20}^{\sigma\sigma}(0) = \frac{-1}{128(x+y-1)^3(2-x-y)^4}(8(4(3y-1)x^5 + 3(16y^2 - 40y + 11)x^4 + 2(36y^3 - 174y^2 + 240y - 67)x^3 + (48y^4 - 364y^3 + 934y^2 - 926y + 249)x^2 + 2(6y^5 - 72y^4 + 280y^3 - 499y^2 + 397y - 100)x - 12y^5 + 73y^4 - 206y^3 + 305y^2 - 216y + 52) - b^2(x+y-3)(x+y-2)^3(x+y-1)^2)$$

$$A_{11}^{\sigma\sigma}(0) = \frac{b}{64(x+y-1)^2(x+y)^3\sqrt{xy}}((1-8y)x^4 + (-24y^2 - 28y + 6)x^3 - (24y^3 + 58y^2 - 34y + 3)x^2 + 2y(-4y^3 - 14y^2 + 17y + 1)x + y^2(y^2 + 6y - 3))$$

$$A_{21}^{\sigma\sigma}(0) = \frac{b}{64(x+y-1)^2(2-x-y)^3\sqrt{(1-x)(1-y)}}((7-8y)x^4 - 2(12y^2 - 54y + 37)x^3 + (-24y^3 + 202y^2 - 430y + 231)x^2 - 2(4y^4 - 54y^3 + 215y^2 - 307y + 134)x + 7y^4 - 74y^3 + 231y^2 - 268y + 100)$$

$$A_{12}^{\sigma\sigma}(0) = \frac{-b^2(x+y+1)}{128(x+y)(x+y-1)}, \qquad A_{22}^{\sigma\sigma}(0) = \frac{b^2(x+y-3)}{128(2-x-y)(x+y-1)}$$

$$B_0^{\sigma\sigma}(0) = \frac{1}{256\pi(x+y)^4(2-x-y)^4(x+y-2xy)^2}(10b^2(2y-1)x^9 + (b^2(336y^2 - 426y + 121) - 128(1-2y)^2)x^8 + 8((198y^3 - 465y^2 + 309y - 59)b^2 + 16(-16y^3 + 40y^2 - 26y + 5))x^7 + 4(b^2(892y^4 - 3170y^3 + 3571y^2 - 1482y + 186) - 32(12y^4 - 80y^3 + 72y^2 - 11y - 3))x^6 + 4((1110y^5 - 5451y^4 + 9006y^3 - 6006y^2 + 1516y - 96)b^2 + 32(32y^5 - 44y^4 - 110y^3 + 45y^2 + 34y - 12))x^5 + 2((1560y^6 - 10230y^5 + 23235y^4 - 22260y^3 + 8620y^2 - 960y - 24)b^2 + 64(68y^6 - 284y^5 + 246y^4 + 203y^3 - 115y^2 - 28y + 12))x^4 + 8y((142y^6 - 1277y^5 + 3947y^4 - 5225y^3 + 2868y^2 - 464y - 24)b^2 + 16(48y^6 - 304y^5 + 730y^4 - 537y^3 - 196y^2 + 168y - 16))x^3 + 4y^2((36y^6 - 570y^5 + 2603y^4 - 4878y^3 + 3782y^2 - 864y - 72)b^2 + 32(12y^6 - 120y^5 + 496y^4 - 967y^3 + 765y^2 - 88y - 24))x^2 - 2y^3((6y^6 + 45y^5 - 612y^4 + 1924y^3 - 2264y^2 + 768y + 96)b^2 + 64(12y^5 - 78y^4 + 281y^3 - 482y^2 + 348y - 48))x + y^4(b^2(6y^3 + 33y^2 - 76y - 12)(y-2)^2 + 128(3y^4 - 15y^3 + 51y^2 - 76y + 44)))$$

$$B_1^{\sigma\sigma}(0) = \frac{-b}{512\sqrt{2}\pi(x+y)^3(2-x-y)^3(x+y-2xy)^{5/2}}(-6b^2(1-2y)^2x^8 - (2y-1)(3b^2(24y^2 - 40y + 11) - 16(32y^2 - 32y + 13))x^7 + (8(512y^4 - 1472y^3 + 1224y^2 - 446y + 61) - 3b^2(120y^4 - 408y^3 + 428y^2 - 161y + 18))x^6 + (16(384y^5 - 1728y^4 + 3318y^3 - 2541y^2 + 863y - 103) - 3b^2(160y^5 - 760y^4 + 1186y^3 - 715y^2 + 148y - 4))x^5 + (8(512y^6 - 3456y^5 + 10480y^4 - 16590y^3 + 11011y^2 - 2982y + 236) - 3b^2(120y^6 - 760y^5 + 1636y^4 - 1417y^3 + 430y^2 - 4y - 8))x^4 + (-16(9b^2 - 64)y^7 + 8(153b^2 - 1472)y^6 + (43616 - 3558b^2)y^5 + (4251b^2 - 109040)y^4 - 24(75b^2 - 5836)y^3 - 8(3b^2 + 8428)y^2 + 96(b^2 + 100)y + 192)x^3 + y(-24b^2y^7 + 24(13b^2 - 64)y^6 + (4672 - 1284b^2)y^5 + 33(65b^2 - 336)y^4 + (42904 - 1290b^2)y^3 - 24(b^2 + 2084)y^2 + 48(3b^2 + 268)y + 576)x^2 + y^2(24b^2y^6 + (672 - 186b^2)y^5 + 3(161b^2 + 816)y^4 - 4(111b^2 + 1796)y^3 + 12(b^2 - 196)y^2 + 32(3b^2 + 140)y + 576)x + y^3(-6b^2y^5 + (33b^2 - 80)y^4 - 6(9b^2 + 196)y^3 + 12(b^2 + 204)y^2 + 24(b^2 - 28)y + 192))$$

$$B_2^{\sigma\sigma}(0) = \frac{b^2}{256\pi(x+y)^2(2-x-y)^2(x+y-2xy)^2}(10(2y-1)x^5 + (256y^2 - 306y + 81)x^4 + 4(110y^3 - 293y^2 + 181y - 27)x^3 + 2(96y^4 - 522y^3 + 619y^2 - 162y - 6)x^2 - 2y(6y^4 + 81y^3 - 282y^2 + 146y + 12)x + y^2(6y^3 + 33y^2 - 76y - 12))$$

$$B_3^{\sigma\sigma}(0) = \frac{b^3(-2y + x(4y-2) - 1)}{512\sqrt{2}\pi(x+y-2xy)\sqrt{x+y-2xy}} \tag{B9}$$

for $\mathcal{T}_{H0}^{\sigma\sigma}(x, y, \mathbf{b}_1, \mathbf{b}_2)$ and

$$A_{10}^{\sigma\sigma}(2) = \frac{1}{64(x+y-1)^3(x+y)^4}(-b^2x^6 + (b^2 + 96y - 64)x^5 + (b^2(9y^2 - 7y + 1) - 8(24y^2 + 36y - 19))x^4 + ((16y^3 - 26y^2 + 10y - 1)b^2 + 24(-24y^3 + 28y^2 + 14y - 3))x^3 + (3(3b^2 - 64)y^4 + (800 - 26b^2)y^3 + 2(9b^2 - 200)y^2 - 3(b^2 + 8)y - 24)x^2 + (96y^5 - (7b^2 + 96)y^4 + 2(5b^2 - 24)y^3 - 3(b^2 - 56)y^2 - 64y + 24)x + y(-b^2y^5 + b^2y^4 + (b^2 - 40)y^3 - (b^2 - 120)y^2 - 88y + 24))$$

$$A_{20}^{\sigma\sigma}(2) = \frac{-1}{64()(x+y-1)^3(2-x-y)^4}(b^2x^6 + (-5b^2 - 96y + 32)x^5 + ((-9y^2 + 11y + 7)b^2 + 24(8y^2 - 8y + 7))x^4 + ((-16y^3 + 58y^2 - 50y + 1)b^2 + 8(72y^3 - 228y^2 + 222y - 79))x^3 + ((-9y^4 + 58y^3 - 114y^2 + 75y - 8)b^2 + 8(24y^4 - 212y^3 + 434y^2 - 301y + 51))x^2 + ((11y^4 - 50y^3 + 75y^2 - 40y + 4)b^2 + 8(-12y^5 + 142y^3 - 229y^2 + 64y + 41))x + b^2y^6 + (96 - 5b^2)y^5 + (7b^2 - 152)y^4 + (b^2 - 56)y^3 - 8(b^2 + 5)y^2 + 4(b^2 + 114)y - 320)$$

$$A_{11}^{\sigma\sigma}(2) = \frac{b}{32(x+y-1)^2(x+y)^3\sqrt{xy}}((8y-1)x^4 - 2(12y^2 + 7y - 3)x^3 + (-24y^3 + 22y^2 + 20y - 3)x^2 + 2y(4y^3 - 7y^2 + 10y - 1)x - y^2(y^2 - 6y + 3))$$

$$A_{21}^{\sigma\sigma}(2) = \frac{b}{32(x+y-1)^2(2-x-y)^3\sqrt{(1-x)(1-y)}}((8y-7)x^4 + (-24y^2 + 30y - 4)x^3 + (-24y^3 + 122y^2 - 146y + 39)x^2 + 2(4y^4 + 15y^3 - 73y^2 + 71y - 13)x - 7y^4 - 4y^3 + 39y^2 - 26y - 4)$$

$$A_{12}^{\sigma\sigma}(2) = \frac{b^2(x^2 - 4yx + x + y^2 + y)}{64(x+y-1)(x+y)^2}, \qquad A_{22}^{\sigma\sigma}(2) = \frac{b^2(x^2 - 4yx + x + y^2 + y)}{64(x+y-1)(2-x-y)^2},$$

$$B_0^{\sigma\sigma}(2) = \frac{1}{128\pi(x+y)^4(2-x-y)^4(x+y-2xy)^2}(10b^2(1-2y)x^9 + ((-72y^2 + 162y - 55)b^2 + 128(1-2y)^2)x^8 + ((192y^3 - 210y + 49)b^2 + 128(160y^3 - 256y^2 + 134y - 23))x^7 + ((1160y^4 - 2992y^3 + 2240y^2 - 765y + 150)b^2 + 128(12y^4 - 584y^3 + 732y^2 - 293y + 36))x^6 + (b^2(1992y^5 - 8460y^4 + 11538y^3 - 6591y^2 + 1868y - 228) - 128(320y^5 - 764y^4 - 290y^3 + 747y^2 - 284y + 30))x^5 + (b^2(1608y^6 - 9804y^5 + 19998y^4 - 16821y^3 + 6250y^2 - 996y + 24) - 128y(68y^5 - 1004y^4 + 2142y^3 - 799y^2 - 124y + 62))x^4 + (128(5b^2 + 96)y^7 - 16(341b^2 + 1600)y^6 + 2(7993b^2 - 35200)y^5 + (196992 - 19541b^2)y^4 + (9960b^2 - 80896)y^3 - 8(247b^2 - 1728)y^2 + 32(3b^2 - 224)y + 1536)x^3 + y(24(5b^2 - 64)y^7 - 96(15b^2 + 128)y^6 + 32(191b^2 + 656)y^5 + (33920 - 11103b^2)y^4 + (8362b^2 - 96768)y^3 - 8(279b^2 - 5824)y^2 + 144(b^2 - 128)y + 4608)x^2 + y^2(12b^2y^7 - 6(29b^2 - 256)y^6 + 6(173b^2 + 640)y^5 - (2845b^2 + 128)y^4 + 4(851b^2 - 5248)y^3 + (33024 - 1380b^2)y^2 + 96(b^2 - 160)y + 4608)x - y^3(6b^2y^6 + (384 - 57b^2)y^5 + (239b^2 + 384)y^4 + (1536 - 470b^2)y^3 + 4(89b^2 - 1088)y^2 - 8(3b^2 - 512)y - 1536))$$

$$B_1^{\sigma\sigma}(2) = \frac{-b}{256\sqrt{2}\pi(x+y)^3(2-x-y)^3(x+y-2xy)^{5/2}}(6b^2(1-2y)^2x^8-(2y-1)(3(16y-5)b^2+16(32y^2-32y+13))x^7 \\ -(3b^2(72y^4-144y^3+64y^2-13y+3)-8(256y^4-64y^3-384y^2+374y-91))x^6+(8(768y^5-2688y^4 \\ +1716y^3+786y^2-940y+179)-3b^2(128y^5-536y^4+650y^3-311y^2+74y-8))x^5+(8(256y^6-2688y^5 \\ +7616y^4-5922y^3+1475y^2-297y+124)-3b^2(72y^6-536y^5+1124y^4-833y^3+221y^2-8y-4))x^4 \\ -(1024y^7+(512-432b^2)y^6+50(39b^2-464)y^5+(71056-2499b^2)y^4+300(3b^2-176)y^3 \\ +16(3b^2+1165)y^2-48(b^2+124)y+864)x^3+y(24b^2y^7-96(b^2-16)y^6-64(3b^2-32)y^5 \\ +3(311b^2-7760)y^4+(56984-663b^2)y^3-48(b^2+751)y^2+24(3b^2+520)y-2592)x^2+y^2(-24b^2y^6 \\ +(78b^2-672)y^5+(39b^2-3024)y^4+(13472-222b^2)y^3+24(b^2-995)y^2+(13472-222b^2)y^3 \\ +24(b^2-995)y^2+16(3b^2+692)y-2592)x+y^3(6b^2y^5+(80-15b^2)y^4-9(b^2-104)y^3 \\ +24(b^2-111)y^2+12(b^2+296)y-864))$$

$$B_2^{\sigma\sigma}(2) = \frac{b^2}{128\pi(x+y)^2(2-x-y)^2(x+y-2xy)^2}((10-20y)x^5+(8y^2+42y-15)x^4+(280y^3-436y^2 \\ +218y-51)x^3+(72y^4-564y^3+466y^2-117y+6)x^2+y(12y^4-102y^3+378y^2-149y+12)x \\ +y^2(-6y^3+33y^2-83y+6))$$

$$B_3^{\sigma\sigma}(2) = \frac{b^3}{256\sqrt{2}\pi(x+y)(2-x-y)(x+y-2xy)\sqrt{x+y-2xy}}((4y-2)x^3+(-16y^2+10y-3)x^2 \\ +(4y^3+10y^2-1)x-y(2y^2+3y+1)) \tag{B10}$$

for $\mathcal{T}_{H2}^{\sigma\sigma}(x, y, \mathbf{b}_1, \mathbf{b}_2)$

APPENDIX C: THE FUNCTION $s(x, b, Q)$ IN THE SUDAKOV FACTOR

In this appendix we present the explicit expression of the exponent $s(x, b, Q)$ appearing in the Sudakov factor. Defining the variables,

$$\hat{q} \equiv \ln\frac{xQ}{\sqrt{2}\Lambda_{\rm QCD}}, \qquad \hat{b} \equiv \ln\frac{1}{b\Lambda_{\rm QCD}}, \tag{C1}$$

the exponent $s(x, b, Q)$ is presented up to next-to-leading-log approximation [43]

$$s(x,b,Q) = \frac{A^{(1)}}{2\beta_1}\left[\hat{q}\ln\left(\frac{\hat{q}}{\hat{b}}\right)-\hat{q}+\hat{b}\right]+\frac{A^{(2)}}{4\beta_1^2}\left(\frac{\hat{q}}{\hat{b}}-1\right)-\left[\frac{A^{(2)}}{4\beta_1^2}-\frac{A^{(1)}}{4\beta_1}\ln\left(\frac{e^{2\gamma_E-1}}{2}\right)\right]\ln\left(\frac{\hat{q}}{\hat{b}}\right)+\frac{A^{(1)}\beta_2}{4\beta_1^3}\hat{q}\left[\frac{\ln(2\hat{q})+1}{\hat{q}} \\ -\frac{\ln(2\hat{b})+1}{\hat{b}}\right]+\frac{A^{(1)}\beta_2}{8\beta_1^3}[\ln^2(2\hat{q})-\ln^2(2\hat{b})]+\frac{A^{(1)}\beta_2}{8\beta_1^3}\ln\left(\frac{e^{2\gamma_E-1}}{2}\right)\left[\frac{\ln(2\hat{q})+1}{\hat{q}}-\frac{\ln(2\hat{b})+1}{\hat{b}}\right] \\ -\frac{A^{(2)}\beta_2}{16\beta_1^4}\left[\frac{2\ln(2\hat{q})+3}{\hat{q}}-\frac{2\ln(2\hat{b})+3}{\hat{b}}\right]-\frac{A^{(2)}\beta_2}{16\beta_1^4}\frac{\hat{q}-\hat{b}}{\hat{b}^2}[2\ln(2\hat{b})+1]+\frac{A^{(2)}\beta_2^2}{432\beta_1^6}\frac{\hat{q}-\hat{b}}{\hat{b}^3}[9\ln^2(2\hat{b})+6\ln(2\hat{b})+2] \\ +\frac{A^{(2)}\beta_2^2}{1728\beta_1^6}\left[\frac{18\ln^2(2\hat{q})+30\ln(2\hat{q})+19}{\hat{q}^2}-\frac{18\ln^2(2\hat{b})+30\ln(2\hat{b})+19}{\hat{b}^2}\right] \tag{C2}$$

where the coefficients β_i and $A^{(i)}$ are

$$\beta_1 = \frac{33-2n_f}{12}, \qquad \beta_2 = \frac{153-19n_f}{24}, \qquad A^{(1)} = \frac{4}{3}, \\ A^{(2)} = \frac{67}{9}-\frac{\pi^2}{3}-\frac{10}{27}n_f+\frac{8}{3}\beta_1\ln\frac{e^{\gamma_E}}{2}, \tag{C3}$$

with γ_E the Euler constant.

The exponent $s(x, b, Q)$ is obtained under the condition that $xQ/\sqrt{2} > 1/b$, i.e. the longitudinal momentum should be larger than the transverse momentum. So $s(x, b, Q)$ is defined for $\hat{q} \geq \hat{b}$, and set to zero for $\hat{q} < \hat{b}$. As a similar treatment, the complete Sudakov factor e^{-S} is set to unity, if $e^{-S} > 1$, in the numerical analysis. This corresponds to a truncation at large k_T, which spoils the on-shell requirement for the light valence quarks. The quark lines with large k_T should be absorbed into the hard-scattering amplitude, instead of the wave functions.

[1] G.P. Lepage and S.J. Brodsky, Phys. Rev. D **22**, 2157 (1980).
[2] N. Isgur and C.H. Llewellyn Smith, Nucl. Phys. **B317**, 526 (1989).
[3] H.N. Li and G. Sterman, Nucl. Phys. **B381**, 129 (1992).
[4] J. Bolz, P. Koll, and G.A. Schuler, Phys. Lett. B **392**, 198 (1997); Eur. Phys. J. C **2**, 705 (1998).
[5] S.J. Brodsky and G.P. Lepage, Phys. Rev. D **24**, 1808 (1981); A. Duncan and A.H. Mueller, Phys. Rev. D **21**, 1636 (1980); P. Kroll and M. Raulfs, Phys. Lett. B **387**, 848 (1996).
[6] Tsung-Wen Yeh, Phys. Rev. D **66**, 014002 (2002); B. Melic, D. Muller, and K. Passek-Kumericki, Phys. Rev. D **68**, 014013 (2003).
[7] S.S. Agaev, Phys. Rev. D **69**, 094010 (2004); **72**, 114010 (2005); **73**, 059902(E) (2006).
[8] F.G. Cao, Y.B. Dai, and C.S. Huang, Eur. Phys. J. C **11**, 501 (1999); Tao Huang and Xing-Gang Wu, Phys. Rev. D **70**, 093013 (2004).
[9] Xing-Gang Wu and Tao Huang, J. High Energy Phys. 04 (2008) 043.
[10] V.M. Belyaev, A. Khodjamirian, and R. Ruckl, Z. Phys. C **60**, 349 (1993); Zheng-Tao Wei and Mao-Zhi Yang, Nucl. Phys. **B642**, 263 (2002).
[11] Han-Wen Huang, Cai-Dian Lu, Toshiyuki Morii, Yue-Long Shen, Ge-Liang Song, and Jin Zhu, Phys. Rev. D **73**, 014011 (2006); Wei Wang, Yu-Ming Wang, De-Shan Yang, and Cai-Dian Lu, Phys. Rev. D **78**, 034011 (2008).
[12] S.J. Brodsky, T. Huang, and G.P. Lepage, in *Particles and Fields-2, Proceedings of the Banff Summer Institute, Banff, Alberta, 1981*, edited by A.Z. Capri and A.N. Kamal (Plenum, New York, 1983), p. 143; Tao Huang, Bo-Qiang Ma, and Qi-Xing Shen, Phys. Rev. D **49**, 1490 (1994).
[13] V.M. Braun and I.B. Filyanov, Z. Phys. C **44**, 157 (1989); **48**, 239 (1990).
[14] P. Ball, J. High Energy Phys. 01 (1999) 010; P. Ball, V.M. Braun, and A. Lenz, J. High Energy Phys. 05 (2006) 004.
[15] Tao Huang, Ming-Zhen Zhou, and Xing-Hua Wu, Eur. Phys. J. C **42**, 271 (2005); Tao Huang, Xing-Hua Wu, and Ming-Zhen Zhou, Phys. Rev. D **70**, 014013 (2004).
[16] J.H. Kuhn, J. Kaplan, and E.G.O. Safiani, Nucl. Phys. **B157**, 125 (1979).
[17] Makiko Nagashima and Hsiang-nan Li, Eur. Phys. J. C **40**, 395 (2005).
[18] M. Beneke and T. Feldmann, Nucl. Phys. **B592**, 3 (2001).
[19] A. Duncan and A.H. Mueller, Phys. Lett. B **93**, 119 (1980).
[20] V.L. Chernyak and A.R. Zhitnitsky, Nucl. Phys. **B201**, 492 (1982).
[21] N.G. Stefanis, W. Schroers, and H.-C. Kim, Phys. Lett. B **449**, 299 (1999).
[22] A. Khodjamirian, T. Mannel, and M. Melcher, Phys. Rev. D **70**, 094002 (2004).
[23] V.M. Braun and A. Lenz, Phys. Rev. D **70**, 074020 (2004).
[24] P. Ball and R. Zwicky, Phys. Lett. B **633**, 289 (2006).
[25] P. Ball and R. Zwicky, J. High Energy Phys. 02 (2006) 034.
[26] P. Ball and R. Zwicky, Phys. Lett. B **625**, 225 (2005).
[27] A. Schmedding and O.I. Yakovlev, Phys. Rev. D **62**, 116002 (2000).
[28] A.P. Bakulev, S.V. Mikhailov, and N.G. Stefanis, Phys. Rev. D **73**, 056002 (2006).
[29] S.S. Agaev, Phys. Rev. D **72**, 114010 (2005).
[30] C. Amsler *et al.* (Particle Data Group), Phys. Lett. B **667**, 1 (2008).
[31] J.Z. Bai *et al.* (BES Collaboration), Phys. Rev. Lett. **81**, 3091 (1998).
[32] H. Nakazawa *et al.* (Belle Collaboration), Phys. Lett. B **615**, 39 (2005).
[33] C. Quigg and J.L. Rosner, Phys. Rep. **56**, 167 (1979).
[34] W. Buchmuller and S.H.H. Tye, Phys. Rev. D **24**, 132 (1981).
[35] M.L. Mangano and A. Petrelli, Phys. Lett. B **352**, 445 (1995).
[36] R. Barbieri, M. Caffo, R. Gatto, and E. Remiddi, Nucl. Phys. **B192**, 61 (1981).
[37] W. Kwong, P.B. Mackenzie, R. Rosenfeld, and J.L. Rosner, Phys. Rev. D **37**, 3210 (1988).
[38] Han-Wen Huang and Kuang-Ta Chao, Phys. Rev. D **54**, 6850 (1996); **56**, 1821(E) (1997).
[39] K.M. Ecklund *et al.* (CLEO Collaboration), Phys. Rev. D **78**, 091501 (2008).
[40] Cai-Dian Lu, Kazumasa Ukai, and Mao-Zhi Yang, Phys. Rev. D **63**, 074009 (2001).
[41] Satoshi Mishima and A.I. Sanda, Prog. Theor. Phys. **110**, 549 (2003).
[42] A. Pich, in *Effective Field Theory*, Proceedings of the Les Houches Summer School, 2007 arXiv:hep-ph/980630.
[43] Hsiang-nan Li, Phys. Rev. D **52**, 3958 (1995).